TEST-TIME LEARNING OF CAUSAL STRUCTURE FROM INTERVENTIONAL DATA

Anonymous authors
Paper under double-blind review

ABSTRACT

Inferring causal structures from interventional data remains a challenging task, especially when the intervention targets are unknown. *Supervised Causal Learning (SCL)* demonstrates strong empirical performance in predicting causal structures by training on datasets with known causal relations and applying the learned models to unseen test data. However, existing *SCL* methods often face inherent generalization challenges and struggle with the diverse intervention settings encountered in *interventional causal discovery* problem. In this work, we propose TICL (Test-time Interventional Causal Learning), a novel approach that follows the *Test-Time Training (TTT) + Joint Causal Inference (JCI)* paradigm to address these challenges of generalization and versatility, respectively. Specifically, TICL employs a self-augmentation technique that generates training data at test time, tailored to the characteristics of the test data, enabling the model to adapt to the inherent biases in the test distribution. Additionally, by integrating the *JCI* framework with *SCL*, TICL replaces the rule-based logic of the standard PC algorithm with a learning-based approach, effectively leveraging self-augmented training data. Extensive experiments on bnlearn benchmarks demonstrate TICL's superiority in multiple aspects of causal discovery and intervention target detection.

1 INTRODUCTION

Causal discovery asks to identify causal relations from data. Supervised Causal Learning (SCL) is an emerging paradigm of causal discovery, and has demonstrated strong empirical performance (Ke et al., 2023b; Lorch et al., 2022; Ma et al., 2022; Dai et al., 2023). The basic idea of SCL is to treat causal discovery as a structured prediction task, where a prediction model takes a data sample as input and outputs predictions about the causal structures behind the input data, such as the causal graph. Such a model is trained using supervised learning techniques, where the training data comprises various causal structures and their associated data samples.

However, existing SCL works have been primarily focusing on causal discovery from *observational data*. On the other hand, experimentation remains the gold standard for discovering causal relations in many application domains (Pearl, 2009; Fisher et al., 1966). *Interventional data*, in particular, allows for the identification of more causal relations with fewer assumptions (Hauser & Bühlmann, 2012). Applying SCL under interventional settings is thus of considerable empirical importance.

Unfortunately, the SCL paradigm faces two main challenges when interventions are involved, particularly if the specific intervention actions are unknown - a common scenario when the interventions are performed by a third party (Eaton & Murphy, 2007a):

- **Versatility:** Different from the observational setting (where there is no intervention thus the problem enjoys a simple and clean formulation), interventional settings may vary widely, including factors such as known / unknown targets, hard / soft interventions, and single / multiple-variable interventions. This diversity complicates learning versatile models, and existing SCL methods (Ke et al., 2023b; Lorch et al., 2022) are typically limited to specific settings (*e.g.*, hard + known). Adapting these methods to more general interventional settings requires non-trivial effort.
- **Generalizability:** As a supervised learning approach, SCL methods fundamentally face the challenge of generalization – models trained on data following a specific distribution (*e.g.*, one generated by a simulator) may perform poorly on real-world test data. The formulation diversity as mentioned above may further exacerbate the generalization issue in the interventional setting.

To address the generalization challenge, we conducted a systematic investigation on Test-Time Training (TTT) technique, an emerging learning paradigm that gives up the attempt of obtaining generalizable model at all, but instead, seeks to train models at test/inference time in an on-the-fly manner such that the model trained is tailored to and responsible only for a specific problem instance. To this end, we explore three key questions: (1) When should training data be acquired? (2) What kind of training data is effective for SCL? (3) How can such data be acquired in our setting? Specifically,

When: We identify two stages within "test time": "accessing test data" and "performing actual testing". Our approach operates between these stages—after accessing test data but before actual testing—by generating free training data, training the model, and using it for final testing.

What: We observe that the *posterior estimation* of causal graphs, $P(\mathcal{G}|\mathcal{D})$, provides highly effective training data. Specifically, we sample causal graphs $(\mathcal{G}_1, \dots, \mathcal{G}_n)$ from $P(\mathcal{G}|\mathcal{D})$ and use forward sampling to generate datasets $(\mathcal{D}_1, \dots, \mathcal{D}_n)$ that are compatible to $(\mathcal{G}_1, \dots, \mathcal{G}_n)$. These paired instances $\langle \mathcal{G}_i, \mathcal{D}_i \rangle$ serve as training data in a process called *self-augmentation*, as shown in Figure 1.

How: We introduce the IS-MCMC algorithm, which constructs a Markov chain over the augmented graph structure space with *intervention constraints*. This approach efficiently samples from the posterior distribution $P(\mathcal{G}|\mathcal{D})$, provided a well-chosen initial state.

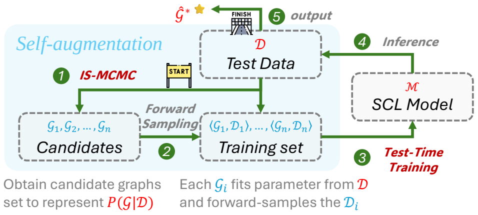

$\hat{\mathcal{G}}^*$
FINISH
5 output
Self-augmentation
$\mathcal{D}$
Test Data
4 Inference
1 IS-MCMC
START
$\mathcal{M}$
SCL Model
Forward Sampling
$\mathcal{G}_1, \mathcal{G}_2, \dots, \mathcal{G}_n$
Candidates
2
$\langle \mathcal{G}_1, \mathcal{D}_1 \rangle, \dots, \langle \mathcal{G}_n, \mathcal{D}_n \rangle$
Training set
3 Test-Time Training
Obtain candidate graphs set to represent $P(\mathcal{G}|\mathcal{D})$
Each $\mathcal{G}_i$ fits parameter from $\mathcal{D}$ and forward-samples the $\mathcal{D}_i$

Figure 1: Self-augmentation strategy.

To address the formulation diversity issue, we advocate to embrace the recently proposed Joint Causal Inference (JCI) technique (Mooij et al., 2020), which pools multiple datasets with unknown interventional targets to create the corresponding augmented data and augmented graphs. Standard causal discovery algorithms can then be applied to this augmented data as if it were purely observational. We observe that the data preprocessing through JCI offers significant convenience for SCL methods, enabling the design of a unified learning task that facilitates causal discovery across diverse interventional settings. Although the JCI technique conveniently unifies various interventional scenarios, enabling SCL, it does not address two critical questions: (1) What should be the appropriate learning target? (2) How should the learning process be designed? Specifically,

What: We value the importance of identifiability in applying SCL to intervention causal discovery, emphasizing that models should predict identifiable causal structures, *i.e.*, $\mathcal{I}$-CPDAG. Directed causal edges are identifiable only when they consistently appear in every causal graph compatible with data.

How: We focus on identifying the identifiable components of the $\mathcal{I}$-CPDAG, namely the skeleton and v-structures. Inspired by the PC algorithm (Spirtes & Glymour, 1991), we adapt it into a two-phase PC-like SCL algorithm for skeleton and orientation learning, ensuring asymptotic correctness while promoting systematic feature characterization and improved classification mechanisms.

By incorporating the above ideas together, we propose a new solution framework, TICL, for the problem of causal discovery from interventional data, focusing on discrete data to illustrate its effectiveness. Specifically, TICL introduces a novel TTT + JCI paradigm, incorporating a self-augmentation algorithm for training data acquisition and a PC-like supervised causal learning algorithm for designing training targets. In summary, our contributions are as follows:

- We propose TICL, a novel TTT + JCI framework for SCL under interventions. Our TICL implementation consistently outperforms existing state-of-the-art methods in experiments.
- We introduce a specific test-time training technique to the SCL domain, which (self-)augments the training data by sampling causal graphs from the posterior distribution via an IS-MCMC process.
- Our systematic study indicates that JCI is a promising direction for interventional causal discovery. It is especially helpful for learning-based methods (which reduce a causal discovery problem into a machine learning problem), thanks to its flexibility in handling various intervention settings.

2 Preliminaries

2.1 Interventional Causal Discovery

A *Causal Graphical Model* (CGM) $\mathcal{M} =< \mathcal{G}, P >$ over d random variables $\mathbf{X} := \{X_1, \dots, X_d\}$ comprises: *(i)* a directed acyclic graph (DAG) $\mathcal{G}$ with nodes corresponding to the variables $\mathbf{X}$ and edges encoding direct causal relations between them, and *(ii)* a joint probability distribution $P_{\mathbf{X}}$ that is *Markov compatible* with $\mathcal{G}$, i.e., $P_{\mathbf{X}} = \prod_{i=1}^{d} P(X_i|pa(X_i))$, where $pa(X_i)$ are the parents of X_i.

Given an unknown causal model $< \mathcal{G}, P >$, the *Observational Causal Discovery* problem asks to infer about the causal graph $\mathcal{G}$ based on an i.i.d. sample of the joint distribution $P_{\mathbf{X}}$. It is however well known that under the observational setting, in the general case, we can only identify a causal graph up to its Markov Equivalent Class (MEC), even if with the *faithfulness assumption* (that $X \perp_P Y|Z \Rightarrow X \perp_{\mathcal{G}} Y|Z$) and with the Markov compatibility condition , where the MEC of the graph $\mathcal{G}$ is the set of graphs with the same *skeleton* and *v-structure*s with $\mathcal{G}$ (Verma & Pearl, 1990).

The identifiability limit in the observational setting can be effectively mitigated by conditioning the observations upon interventions, *i.e.*, actions that purposefully perturb the causal model. In general, an intervention can apply to a subset of variables $I \subset \mathbf{X}$, called the *intervention targets*, which can either be a single variable or contain multiple variables. For each target variable X_i in I, the intervention replaces the conditional distribution $P(X_i|pa(X_i))$ with a new one: $P^{(I)}(X_i|pa(X_i))$. The joint distribution after the intervention thus becomes $P_{\mathbf{X}}^{(I)} = \prod_{i \notin I} P(X_i|pa(X_i)) \prod_{j \in I} P^{(I)}(X_j|pa(X_j))$. The intervention is called a *hard* (*a.k.a. perfect, structural*) *intervention* (Eaton & Murphy, 2007b) if it eliminates the intervention targets' causal dependence on their parents entirely, i.e., if $P^{(I)}(X_i|pa(X_i)) = P^{(I)}(X_i), \forall X_i \in I$; otherwise it is called a *soft* (*a.k.a. imperfect, parametric*) *intervention* (Tian & Pearl, 2001) as it maintains at least part of the original causal dependence. It is an *unknown intervention* if the target set I is unknown.

The *Interventional Causal Discovery* problem asks to infer about the causal graph $\mathcal{G}$ based on a collection of data samples $\mathcal{D} = \{D_0, D_1, \ldots, D_K\}$, each obtained under a different intervention. Let $\mathcal{I} := \{I_0, I_1, \ldots, I_K\}$ be the intervention targets for each of the interventions here. $\mathcal{I}$ is called the *intervention family* of the dataset $\mathcal{D}$. It is often useful to obtain D_0 as a sample of the observational distribution $P_{\mathbf{X}}$ without any actual intervention, and in this case we denote $I_0 = \emptyset$. In this paper, we consider the situation that the interventions are unknown, and we need to infer both about the causal graph $\mathcal{G}$ and about the intervention family $\mathcal{I}$ from the given data collection $\mathcal{D}$.

2.2 Joint Causal Inference

Our method is based on the JCI framework, proposed by Mooij et al. (Mooij et al., 2020), which reduces an interventional causal discovery problem into an observational causal discovery problem over an augmented causal model. The basic idea is to treat a data sample under intervention as an observation under an imposed condition. The data-sample collection $\mathcal{D}$ in the intervention setting can then be seen as a single data sample under a variety of observation conditions. More specifically,

Augmented Data: Given data collection $\mathcal{D} = \{D_0, D_1, \ldots, D_K\}$ obtained under intervention family $\mathcal{I} := \{I_0, I_1, \ldots, I_K\}$, an *augmented data sample* $D_{\mathcal{I}}$ can be constructed by stacking the $K + 1$ data samples in $\mathcal{D}$ together by rows, then appending K columns, each corresponding to a newly added *environment variable* (or *intervention variable*) X_{I_k} which takes binary value and $X_{I_k} = 1$ in and only in data points (= rows) originally from D_k. See the data table in Figure 3 above for illustration.

Augmented Graph: Accordingly, an *augmented causal graph* $\mathcal{G}_{\mathcal{I}}$ can be constructed by adding nodes X_{I_k}, and adding edges $X_{I_k} \rightarrow X_i$ for all $X_i \in I_k$ if the intervention targets I_k are known. In the augmented graph, nodes corresponding to the original variables $X_i \in \mathbf{X}$ are called *system nodes*, and those corresponding to X_{I_k} are called *environment nodes*.

In the JCI framework, we first convert the data collection $\mathcal{D}$ into the augmented data sample $D_{\mathcal{I}}$, optionally incorporating edges from known interventions $\mathcal{I}$, then infer the augmented graph $\mathcal{G}_{\mathcal{I}}$, which encodes both the information of the original causal graph $\mathcal{G}$ over the system variables $\mathbf{X}$, and reveals unknown intervention targets as edges from environment nodes to system nodes are identified.

Moreover, the causal inference over the augmented graph in the JCI framework may be facilitated by some *a priori* constraints when prior knowledge/assumptions about the interventions are available. For example, under the *exogeneity* assumption, the interventions were selected and conducted without conditioning on any system variable $X_i \in \mathbf{X}$, corresponding to a constraint that there should be no causal edges from system nodes to environment nodes. Under the *complete randomized context* assumption, there should be no confounding relation between any system variable/node and any intervention variable/node. Under the *generic context* assumption, there should be no causation between intervention variables/nodes. For more details, please refer to the paper (Mooij et al., 2020).

2.3 Identifiability with Intervention Data

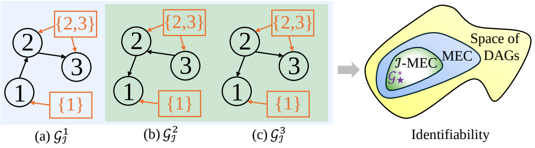

(a) $\mathcal{G}^1_\mathcal{I}$ (b) $\mathcal{G}^2_\mathcal{I}$ (c) $\mathcal{G}^3_\mathcal{I}$ Identifiability

Figure 2: Identifiability Example.

Two causal DAGs $\mathcal{G}_1$ and $\mathcal{G}_2$ are indistinguishable under an intervention family $\mathcal{I}$ with $I_0 = \emptyset$ if and only if their interventional graphs $\mathcal{G}^1_{I_k}$ and $\mathcal{G}^2_{I_k}$ have the same skeleton and v-structures for all $I_k \in \mathcal{I}$ (Yang et al., 2018). It is thus clear that with interventional data, we may identify the true causal graph up to a smaller equivalence class – called the $\mathcal{I}$-MEC. Figure 2 gives a simple example that illustrates how interventions can help with causal identifiability: The three DAGs on the left belong to the same MEC. Considering the intervention family $\mathcal{I} = \{\emptyset, \{1\}, \{2, 3\}\}$, $G^1_\mathcal{I}$ is not in the same $\mathcal{I}$-MEC as $G^2_\mathcal{I}$ and $G^3_\mathcal{I}$ due to the absence of the v-structure $X_2 \to X_1 \leftarrow \{1\}$. The schematic on the right further elucidates the relationships among the true DAG $\mathcal{G}^\star$, the $\mathcal{I}$-MEC, the MEC, and the space of all possible DAGs.

3 TICL: Test-Time Learning of Causal Strcture

In this section, we present the details of TICL method (see Figure 3). We first formally summarize the problem and outline its solution, then delve into the two essential components of our TICL — the *self-augmentation strategy* and *PC-like supervised causal learning*.

Problem Summary. We are given a data collection $\mathcal{D}$, which is obtained from an unknown causal model $(\mathcal{G}, P)$ under an intervention family $\mathcal{I}$. The interventions may be multi-variable, soft, and unknown. We assume i) P is *Markovian* and faithful w.r.t. the causal graph and causal sufficiency, and ii) exogeneity, complete-randomized-context, and generic-context property for the intervention family. These assumptions are standard and natural in the interventional causal discovery domain. We aim to predict all causal relations entailed by the given data $\mathcal{D}$ (subject to the above assumptions), which correspond to the *invariant* causal structures in the $\mathcal{I}$-MEC set of the causal graph $\mathcal{G}$ behind $\mathcal{D}$, as explained in Section 2. Such invariant causal structures can be computationally encapsulated as a partial DAG, called the Interventional-Complete Partial Directed Acyclic Graph ($\mathcal{I}$-CPDAG), in which each directed edge indicates an invariant causal relation in the $\mathcal{I}$-MEC set. Besides the $\mathcal{I}$-CPDAG Discovery task thus discussed, we also want to identify the unknown intervention targets in the intervention family $\mathcal{I}$ (Intervention Target Detection).

Solution Outline. ***(Step 1)*** Following the JCI protocol, our method first converts the given interventional data collection into an augmented observational data sample $\mathcal{D}_\mathcal{I}$. ***(Step 2)*** Then, we use the proposed self-augmentation strategy to construct a Markov chain over the space of augmented graph structures constrained by interventions, where each $\mathcal{G}_i$ fits the parameters in $\mathcal{D}_\mathcal{I}$, and perform forward sampling to get $\mathcal{D}_i$ as the training instance. ***(Step 3)*** Lastly, we modify the rule-based logic of the standard PC algorithm into a learning-based approach, enabling the learning of both the skeleton model and the orientation model by utilizing the self-augmented training data. The former can further identify intervention targets using JCI priors, *i.e.*, prior knowledge of relationship between system variable and environment variable.

3.1 Test-Time Training Data Acquisition via Self-Augmentation

We propose leveraging the posterior estimation of causal graphs, $P(\mathcal{G}_\mathcal{I}|\mathcal{D}_\mathcal{I})$ to generate training data. Specifically, we sample causal graphs $(\mathcal{G}_1, \dots, \mathcal{G}_n)$ from $P(\mathcal{G}_\mathcal{I}|\mathcal{D}_\mathcal{I})$ using a tailored Markov Chain Monte Carlo (MCMC) designed for interventional data. For each $\mathcal{G}_i$, the parameters governing the conditional distributions of variables, given their parents in $\mathcal{G}_i$, are re-estimated using the dataset $\mathcal{D}$. Forward sampling is then applied from $\mathcal{G}_i$ with the re-estimated parameters to produce a new dataset $\mathcal{D}_i$, which is compatible with $\mathcal{G}_i$. These paired instances $\langle \mathcal{G}_i, \mathcal{D}_i \rangle$ are used as training data.

We argue that this augmented training data offers two key advantages: First, since the true causal graph $\mathcal{G}^*$ is unknown, the posterior estimation $(\mathcal{G}_1, \dots, \mathcal{G}_n)$ provides a diverse range of plausible causal structures, capturing epistemic uncertainty. Second, by re-estimating the parameters and forward sampling fully compatible datasets $\mathcal{D}_i$ from each $\mathcal{G}_i$, we generate accurately labeled instances $\langle \mathcal{G}_i, \mathcal{D}_i \rangle$, where $\mathcal{G}_i$ is likely to maintain a certain ”similarity” with the original agumented graph $\mathcal{G}_\mathcal{I}$, which entails the similarity properties of the data $\mathcal{D}_i$. Our experiments demonstrate that these steps are crucial for generating high-quality training data. The key steps are summarized below:

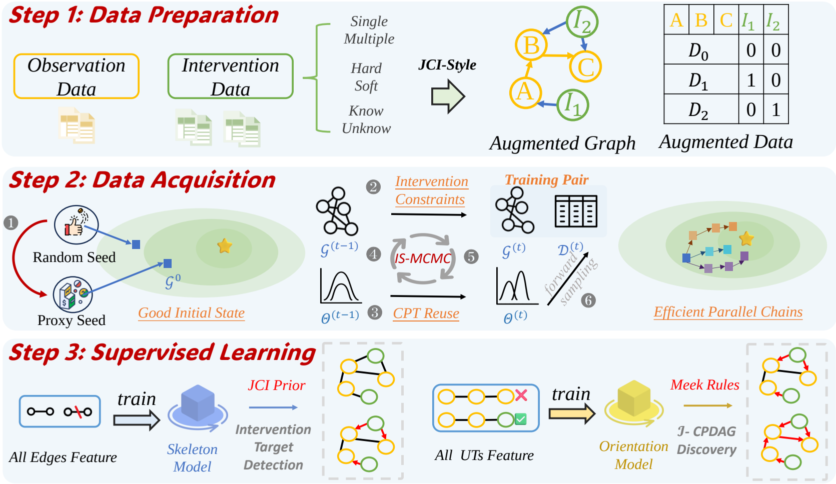

Figure 3: The overall workflow of TICL.

❶ **Initialization**: The initial graph $\mathcal{G}^{(0)}$ is generated using either a proxy algorithm or random initialization.

❷ **Mutation**: In each iteration, a candidate graph $\mathcal{G}^{cand}$ is generated from $\mathcal{G}^{(t-1)}$ by mutating the structure (adding, deleting, or reversing an edge).

❸ **Parameters Re-Estimation**: For each $\mathcal{G}^{cand}$, the conditional probability table (CPT) is re-estimated via maximum likelihood estimation (MLE), ensuring alignment with the augmented data $\mathcal{D}_{\mathcal{I}}$. If a node's parents remain unchanged, the corresponding CPT is inherited from the previous graph.

❹ **Evaluation**: The candidate graph $\mathcal{G}^{cand}$ is evaluated using a goodness-of-fit score, such as log-likelihood, computed based on its alignment with the observed data.

❺ **Acceptance**: The acceptance probability of G^{cand} is computed as: $\alpha(\mathcal{G}^{cand}|\mathcal{G}^{(t-1)}) = \min\left(1, \frac{\text{score}(\mathcal{G}^{cand})}{\text{score}(\mathcal{G}^{(t-1)})}\right)$, $\mathcal{G}^{cand}$ is accepted as $\mathcal{G}^{(t)}$ with probability α, otherwise it retains $\mathcal{G}^{(t-1)}$.

❻ **Forward Sampling**: Once $\mathcal{G}^{cand}$ is accepted, the corresponding dataset $\mathcal{D}^{(t)}$ is generated by forward sampling from the graph, and the pair $\langle \mathcal{G}^{(t)}, \mathcal{D}^{(t)} \rangle$ is stored for future use.

Further Optimization Considerations

There are, however, two critical considerations that need to be addressed. First, since the IS-MCMC process operates on augmented graphs rather than standard causal graph, additional constraints must be taken to ensure the validity of the process. More importantly, managing the time complexity of this process is crucial to maintaining efficient inference.

▷ **Good Initial State**: Using a proxy algorithm to generate an inital graph significantly reduces convergence time compared to starting from a random graph.

▷ **Efficient Parallel Chains**: Running multiple parallel IS-MCMC chains allows for faster exploration of the graph space, improving the efficiency.

▷ **Intervention Constraints**: The mutation process must respect system-environment (*sys node* – *env node*) constraints that are specific to the interventional setup. Specifically, edges from system to environment nodes (*sys* → *env*) are not permitted, and interactions between environment nodes are excluded. This ensures that the augmented graphs remain consistent under the JCI framework.

▷ **Parameters Reuse**: Only the nodes affected by structural changes need to have their CPTs re-estimated. The rest of the graph can retain its parameters from the previous iteration.

By addressing these factors, we ensure that the process of generating training data at test time is both effective and efficient, leading to improved performance in causal discovery under interventional settings. This process is detailed in Algorithm 1, where the key optimization strategies are highlighted.

Algorithm 1 IS-MCMC Algorithm Workflow

```
❶ Initialize Seed Graph with Proxy Algorithm: $\mathcal{G}^{(0)} \leftarrow \text{proxy}(\mathcal{D}_{\mathcal{I}})$    ▷ Good Initial State
  Estimating CPT parameters by maximum likelihood: $\Theta^{(0)} = \text{MLE}(\mathcal{G}^{(0)}, \mathcal{D}_{\mathcal{I}})$
Parallel $i \in 1, 2, \dots, N$ do:    ▷ Efficient Parallel Chains
  for iteration $t = 1, 2, \dots, L$ do:
    ❷ Propose: $\mathcal{G}^{cand} \sim q(\mathcal{G}^{(t)} \mid \mathcal{G}^{(t-1)})$ with Intervention Constraint.    ▷ Intervention Constraints
    ❸ Re-parameterize according to the previous graph ( B.1.1): $\Theta^{cand} = \text{Estimation}(\mathcal{G}^{cand}, \Theta^{(t-1)})$    ▷ Parameters Reuse
    ❹ Calculate Acceptance Probability:$\alpha(\mathcal{G}^{cand} \mid \mathcal{G}^{(t-1)}) = \min\left\{1, \frac{q(\mathcal{G}^{(t-1)}|\mathcal{G}^{cand})P(\mathcal{G}^{cand}|\mathcal{D}_{\mathcal{I}})}{q(\mathcal{G}^{cand}|\mathcal{G}^{(t-1)})P(\mathcal{G}^{(t-1)}|\mathcal{D}_{\mathcal{I}})}\right\}$
    ❺ Randomly Sample: $u \sim \text{Uniform}[0, 1]$
      Accept proposal: $\mathcal{G}^{(t)} \leftarrow \mathcal{G}^{cand}, \Theta^{(t)} \leftarrow \Theta^{cand}$ if $u < \alpha$ else Reject proposal: $\mathcal{G}^{(t)} \leftarrow \mathcal{G}^{t-1}, \Theta^{(t)} \leftarrow \Theta^{(t-1)}$
  ❻ Forward Sampling data: $\mathcal{D}^{(t)} \leftarrow \text{Sampling}(\mathcal{G}^{(t)}, \Theta^{(t)})$
```

3.2 PC-LIKE SUPERVISED CAUSAL LEARNING

We first consider a two-phase, PC-like process for causal discovery, consisting of skeleton detection and orientation. The first phase detects the skeleton and identifies interventional targets, while the second phase orients a directed acyclic graph that is identifiable up to an $\mathcal{I}$-MEC. Notably, we propose that both phases can be transitioned from rule-based logic to a learning-based approach, allowing the application of supervised learning methods. This shift implies that for each phase, we must define the learning target, the feature set, and the classification mechanism.

Revisiting the PC Algorithm. The PC algorithm consists of two main phases: Phase 1 identifies the skeleton and the separating sets $\mathcal{SS}$, determining the existence of edges. Starting from an undirected complete graph, edges are removed iteratively through conditional independence (CI) tests. Specifically, an edge $X_i - X_j$ is removed if X_i is conditionally independent of X_j given a subset $\mathcal{S}$ of other variables in the current k-order graph. Phase 2 orients the unshielded triples in the skeleton based on the separating sets, assigning edge directionality. For example, the triple $\langle X_a, X_c, X_b \rangle$ is oriented into a v-structure $X_a \rightarrow X_c \leftarrow X_b$ if X_c is not in the separating set of X_a and X_b.

Connecting PC and Supervised Learning. We now establish a formal connection between PC and SCL. Due to limited space, we focus on phase 2 as an example. Further details are provided in B.2.

Task: For all unshielded triples $\mathcal{U}$, classify whether each triple $\langle X_a, X_c, X_b \rangle$ is a v-structure.

Featurization: Query all separating sets $\mathcal{SS}$ satisfying $X_a \perp X_b | \mathcal{SS}$, and calculate existence feature:

$$F_{\langle X_a, X_c, X_b \rangle} = \begin{cases} 1 & X_c \in \mathcal{SS} \\ 0 & X_c \notin \mathcal{SS} \end{cases}$$

Classifier: Train a binary classifier using features:

$$C_{orientation}(F_{\langle X_a, X_c, X_b \rangle}) := \begin{cases} \textit{v-structure} & F_{\langle X_a, X_c, X_b \rangle} \neq 0 \\ \textit{non-v-structure} & F_{\langle X_a, X_c, X_b \rangle} = 0 \end{cases}$$

In summary, detecting v-structures can be framed as a binary classification task, with the PC algorithm viewed as a form of feature engineering combined with a static classifier. It's clear that this approach can be extended by enriching the feature set, such as considering all possible separating sets or gathering more conditional dependency information. Crucially, it also enables us to replace heuristic searches and potentially erroneous CI tests with robust classification mechanism trained on our data.

Prior Knowledge by Augmented Graph

Building on this framework, we introduce two classifiers: one to detect the existence of edges between nodes, and the other to determine whether an unshielded triple is a v-structure. Details of the feature set we propose can be found in appendix B.2.3. Additionally, the interventional setting—specifically, the augmented graph—offers further advantages. During inference, prior knowledge from the augmented graph allows us to pre-identify certain edges (e.g., (*environment node* → *system node*)), facilitating the application of Meek rules (Meek, 1995) to identify additional edges.

4 Experiments

In this section, we conduct extensive experiments to answer the following research questions:

RQ1: How does the `TICL` perform in intervention target detection and causal discovery from interventional data? ***(Effectiveness)***.

RQ2: How does the quality and quantity of training data generated by `IS-MCMC` affect supervised causal discovery? ***(Generalizability)***.

RQ3: How about the computational complexity of our method? ***(Efficiency)***.

RQ4: How does the JCI framework benefit the uniformity and performance of our supervised causal approach `TICL` across different intervention settings? ***(Versatility)***.

Benchmarks & Baselines. We use 14 semi-real causal graph datasets collected from the bnlearn (Scutari, 2010) repository as benchmarks. To address the research questions, we compare our `TICL` with methods[1] specifically designed for intervention data, including score-based methods such as GIES (Hauser & Bühlmann, 2012), IGSP (Wang et al., 2017; Yang et al., 2018), UT-IGSP (Squires et al., 2020), and continuous optimization-based methods like ENCO (Lippe et al., 2022), AVICI (Lorch et al., 2022). Additionally, considering the generality of the JCI framework (Mooij et al., 2020), we further extend the existing causal discovery methods of purely observational data combined with the JCI framework to intervention settings, encompassing constraint-based methods such as PC (Spirtes & Glymour, 1991), score-based methods like HC (Tsamardinos et al., 2006), BLIP (Scanagatta et al., 2015), and gradient-based methods such as GOLEM (Ng et al., 2020).

Training Datasets & Metrics. For the training data, we use 400 synthetic causal graph instances sampled via the `IS-MCMC` method, concurrently employing forward sampling of 10,000 samples from re-parameterized conditional probability tables as training instances. We employ XGBoost (Chen & Guestrin, 2016) as the classifier with default parameters to train the model. The F1-Score is used to evaluate intervention target detection as well as the $\mathcal{I}$-*CPDAG* discovery. Additionally, for the latter, we employ two standard metrics for causal assessment: Structural Hamming Distance (SHD) and Structural Intervention Distance (SID) (Peters & Bühlmann, 2015). More detailed settings are provided in Appendix E.

4.1 Causal Structure Identification and Intervention Target Detection (RQ1)

Following GIES (Hauser & Bühlmann, 2012) and DCDI (Brouillard et al., 2020), for each graph, we conduct multiple intervention experiments, with the number of experiments equaling twenty percent of the number of nodes. In each intervention experiment, to enhance the diversity of the baseline, we employ single-node interventions (*e.g.* ENCO method limited to single-node interventions). As hard interventions can be considered a special case of soft interventions, we opt for soft intervention measures. Then, we forward-sample 10,000 samples for both observational cases and each intervention experiment to obtain the test data.

As shown in Table 1 and Table 2, `TICL` achieves competitive results across all evaluation metrics on 14 different causal graph datasets. We highlight its advantages in two key aspects: ❶ **Multi-Scale and Diverse Benchmarking:** Unlike recent methods (Brouillard et al., 2020; Lorch et al., 2022; Hägele et al., 2023; Ke et al., 2023b) that are tested only on synthetic datasets with 10-30 nodes, we evaluate on the diverse bnlearn benchmark, which includes causal graphs inspired by real-world applications with scales ranging from small to even over 100 nodes. Given that the number of DAGs grows exponentially with the number of nodes, most methods fail or timeout, while our experiments demonstrate superior scalability and consistent performance. ❷ **Highly Competitive Results:** In the intervention target detection task, our performance significantly surpasses all other methods, with the F1 score improving by an average of 50.21% over the second-best method across the 14 datasets. Furthermore, the F1 score of $\mathcal{I}$-*CPDAG* discovery shows an average improvement of 13.62% over

[1] Note that some methods cater only to specific intervention settings. We adjust them for the corresponding experiments, marked with *. Additionally, DCDI (Brouillard et al., 2020) and BaCaDI (Hägele et al., 2023) failed in experiments due to their focus on continuous data, and the inaccessible or uncompileable source code of CSIvA (Ke et al., 2023b) and SDI (Ke et al., 2023a) lead us to omit reporting their results. We provide more discussions and comparisons with related work in Appendix E.2.

Table 1: Performance comparison of *I-CPDAG* (SHD ↓ / SID ↓ / F1-Score ↑). ♣: Crashes, ♠: Timeout. 🟩 JCI-Improved baseline. 🟦 Modified adaptation baseline (Intervention targets that can be known). 🟧 Classical baselines. **Blue** means best, underline means second best.

Methods	TICL			JCI-PC			JCI-BLIP			JCI-HC			JCI-GOLEM			AVICI*			ENCO*			IGSP*			UT-IGSP			GIES		
	SHD	SID	F1	SHD	SID	F1	SHD	SID	F1	SHD	SID	F1	SHD	SID	F1	SHD	SID	F1	SHD	SID	F1	SHD	SID	F1	SHD	SID	F1	SHD	SID	F1
Earthquake	**0**	**0**	**1.00**	**0**	**0**	**1.00**	**0**	**0**	**1.00**	5	14	0.40	6	19	0.00	3	6	0.40	3	12	0.67	**0**	**0**	**1.00**	**0**	**0**	**1.00**	1	**0**	0.89
Survey	**0**	**0**	**1.00**	5	18	0.40	1	4	0.91	**0**	**0**	**1.00**	7	23	0.40	8	18	0.22	5	21	0.29	1	4	0.91	1	4	0.91	1	4	0.91
Asia	**2**	**13**	**0.86**	4	19	0.75	3	18	0.77	6	28	0.46	15	36	0.00	7	28	0.31	6	**13**	0.74	4	17	0.62	5	24	0.73	4	14	0.77
Sachs	**3**	**6**	**0.90**	19	56	0.52	7	41	0.67	5	29	0.74	18	61	0.11	37	46	0.22	41	42	0.26	10	16	0.70	13	21	0.61	15	38	0.48
Child	**7**	**67**	**0.81**	40	299	0.62	10	188	0.78	16	211	0.65	41	330	0.21	♣	♣	♣	110	251	0.06	29	124	0.63	33	214	0.45	46	197	0.29
Insurance	**17**	295	**0.78**	66	537	0.53	24	360	0.68	32	342	0.60	63	687	0.23	♣	♣	♣	172	505	0.14	80	455	0.34	82	442	0.31	87	**261**	0.52
Water	**45**	**470**	**0.53**	♠	♠	♠	46	538	0.49	48	503	0.46	81	564	0.22	♣	♣	♣	58	527	0.46	♣	♣	♣	♣	♣	♣	♣	♣	♣
Mildew	**29**	239	**0.76**	58	766	**0.76**	35	523	0.51	41	500	0.51	♠	♠	♠	♣	♣	♣	262	820	0.10	130	482	0.22	123	430	0.25	116	**81**	0.41
Alarm	**9**	**96**	**0.91**	67	481	0.76	18	152	0.75	38	416	0.61	♠	♠	♠	♣	♣	♣	236	612	0.11	65	247	0.43	70	274	0.37	88	219	0.39
Barley	55	948	0.63	127	1789	0.57	**39**	**919**	**0.70**	78	1328	0.39	♠	♠	♠	♣	♣	♣	98	1059	0.55	♣	♣	♣	♣	♣	♣	♠	♠	♠
Hailfinder	**42**	**509**	0.66	157	1152	0.33	43	558	**0.70**	81	935	0.38	♠	♠	♠	♣	♣	♣	98	730	0.61	232	870	0.14	235	910	0.14	66	973	0.00
Hepar2	**42**	1216	0.79	♠	♠	♠	50	1228	0.72	43	**855**	**0.81**	♠	♠	♠	♣	♣	♣	75	1693	0.57	70	1663	0.62	67	1606	0.64	81	1085	0.67
Win95pts	**101**	**611**	**0.58**	♠	♠	♠	109	900	0.53	♠	♠	♠	♠	♠	♠	♣	♣	♣	135	893	0.54	♣	♣	♣	♣	♣	♣	112	992	0.00
Pathfinder	187	9473	0.27	♠	♠	♠	207	♣	0.30	♠	♠	♠	♠	♠	♠	♣	♣	♣	**156**	**5528**	**0.47**	1345	7261	0.10	1348	9226	0.08	♠	♠	♠
Rank (SHD)	**1.14 ± 0.12**			5.36 ± 3.23			2.14 ± 0.41			3.86 ± 4.41			7.43 ± 3.67			8.07 ± 2.78			6.36 ± 5.80			4.64 ± 2.66			5.21 ± 2.74			5.50 ± 3.11		
Rank (SID)	**1.57 ± 0.82**			6.43 ± 3.82			3.57 ± 2.53			4.64 ± 5.37			8.14 ± 3.69			7.64 ± 2.66			5.29 ± 7.92			3.93 ± 2.78			4.57 ± 2.67			3.43 ± 2.96		
Rank (F1)	**1.36 ± 0.37**			4.43 ± 4.24			2.29 ± 0.78			3.93 ± 4.49			7.71 ± 3.35			8.00 ± 3.14			5.93 ± 7.49			4.86 ± 2.84			5.21 ± 2.45			5.36 ± 2.52		

Table 2: Performance comparison of *Intervention Targets Detection* (F1-Score ↑).

Datasets	**Earthquake**	**Survey**	**Asia**	**Sachs**	**Child**	**Insurance**	**Water**	**Mildew**	**Alarm**	**Barley**	**Hailfinder**	**Hepar2**	**Win95pts**	**Pathfinder**	**Rank** (F1)
UT-IGSP	0.50	**1.00**	0.44	0.33	0.35	0.17	♣	0.22	0.15	♣	0.27	0.23	♣	0.04	5.14±3.27
CITE	**1.00**	**1.00**	0.67	0.36	0.67	0.32	♣	0.38	0.56	♣	0.67	0.61	♣	0.60	3.07±2.21
PreDITEr	**1.00**	**1.00**	0.67	0.50	♠	♠	♣	♠	♠	♣	♠	♠	♣	♣	5.21±5.17
JCI-GOLEM	0.67	0.40	0.40	0.22	0.18	0.11	0.23	♠	♠	♠	♠	♠	♠	♠	6.29±2.20
JCI-HC	**1.00**	0.50	0.67	0.57	0.40	0.29	0.33	0.34	0.29	0.26	0.23	0.23	♠	♠	4.14±1.98
JCI-BLIP	**1.00**	**1.00**	0.80	0.67	0.57	0.45	0.44	0.35	0.38	0.34	0.34	0.82	0.29	0.23	2.43±0.67
JCI-PC	**1.00**	**1.00**	0.80	0.57	0.28	0.50	♠	0.26	0.64	0.70	0.25	♠	♠	♠	3.43±3.10
TICL	**1.00**	**1.00**	**1.00**	**1.00**	**1.00**	**0.83**	**0.86**	**0.58**	**0.82**	**0.83**	**0.76**	**0.90**	**0.50**	**0.74**	**1.00±0.00**

the best baseline on these datasets. One exception is ENCO on the Pathfinder, where comparable performance is due to the provision of prior knowledge of known intervention targets. Finally, we also observe that methods based on the JCI framework achieve competitive performance in both tasks, indicating that JCI is a promising direction for intervention causal discovery. Overall, TICL stands out among all these competitors, with an average-F1 rank of 1.36 ± 0.37 for causal discovery and 1.00 ± 0.00 for intervention target detection.

4.2 Training Data Study in SCL: Quantity and Quality (RQ2)

We maintain consistent intervention experimental setups and further assess the impact of pre-generated synthetic training data quality and quantity on supervised causal learning across different graphs.

Data Quality. To evaluate the influence of training data quality, we consider three different training data generation strategies: *Purely Random*, wherein random graphs (Erdős-Rényi model (Erdős et al., 1960) and Scale-Free model (Albert & Barabási, 2002)) with a probability distribution sampled from a Dirichlet distribution with parameter $\alpha \sim U[0.1, 1.0]$ are generated as training data, with node sizes ranging from 10 to 50; IS−MCMC *w/ Random Seed*, where random graphs with node sizes equal to those of the augmented graphs are generated as the initial seed graph while IS−MCMC simulations are performed; and IS−MCMC *w/ Proxy Seed*, which involves utilizing proxy algorithms (*e.g.*, JCI-BLIP) to generate the initial seed graph combined with IS−MCMC simulations as training data. As shown in Figure 4, we first compare the performance of three strategies on different datasets. Second, we study the convergence of IS−MCMC sampling for the two strategies, as shown in Figure 5. We observe that:

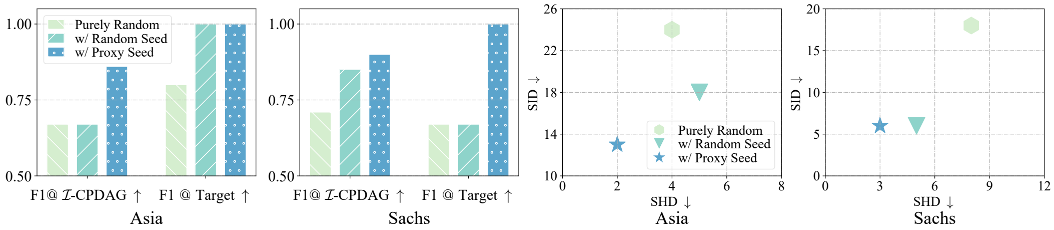

Figure 4: Experimental results of different strategies for generating synthetic training data.

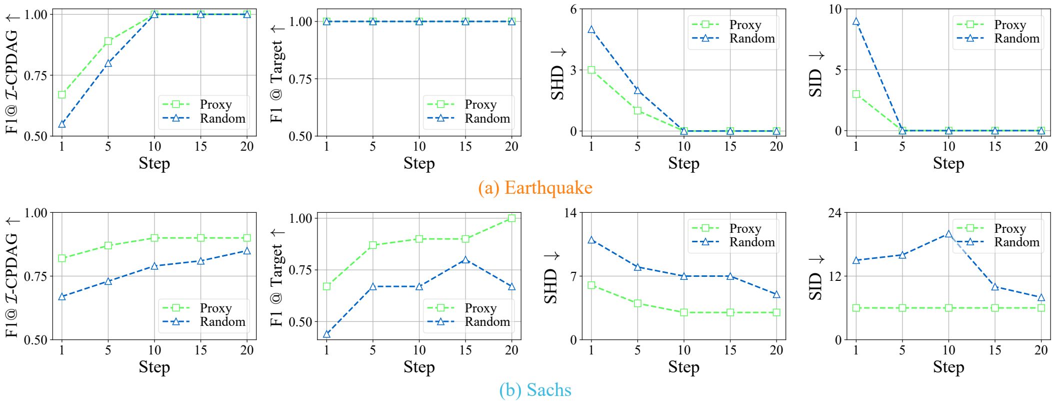

(a) Earthquake

(b) Sachs

Figure 5: Experimental results of convergence comparison of different IS−MCMC strategies.

Obs.➊ High-quality in-domain training data is crucial for supervised causal model. The three aforementioned data generation strategies can be viewed as progressively approaching the testing data domain. As depicted in Figure 4, the training data generated by the two strategies utilizing IS−MCMC exhibit superior performance across various metrics of the different network compared to the purely random strategy. Among them, employing the proxy seed method yields the best performance, which illustrates the importance of the effective starting point we proposed.

Obs.➋ Under in-domain generation, posterior distribution induce training data is the key of self-augmentation for IS−MCMC. While both IS−MCMC strategies aim for the same posterior distribution, empirical studies show that initial seeds produced by proxy algorithms frequently exhibit faster convergence and achieve better results in causal discovery and intervention target detection than random seeds, as depicted in Figure 5. This also demonstrates the efficiency of our starting point strategy on the TICL and the faster achievement of the goal.

Data Quantity. We evaluate the scaling law intuition between the performance of supervised causal models TICL and the training data size from two aspects: the number of training data instances and the sample size of each instance. Figure 6 provides an overview of the impact of varying scales of training data instances on performance. Figure 7 outlines the training of TICL on training data of different sample sizes: specifically, 2k, 5k, 10k, and 20k, and the performance of inference under default intervention experiment settings. We offer the following observations:

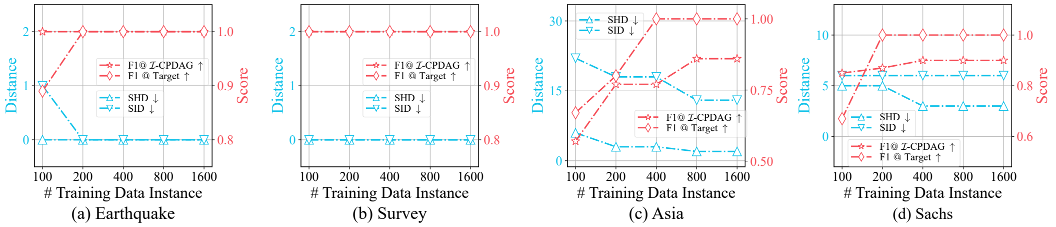

(a) Earthquake

(b) Survey

(c) Asia

(d) Sachs

Figure 6: The impact of different scales of training data instances on performance.

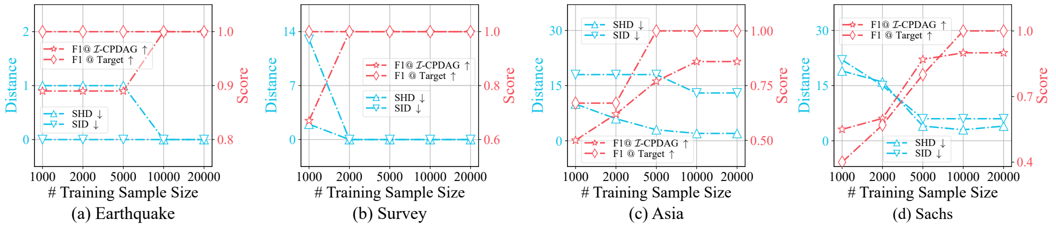

(a) Earthquake

(b) Survey

(c) Asia

(d) Sachs

Figure 7: The impact of different training sample sizes on performance.

Obs.➊ Our TICL benefits from the size of training data instances. More specifically, as depicted in Figure 6, with the continuous increase in the number of training data instances, the performance of TICL consistently improve across all datasets. In smaller networks, a small amount of data is sufficient to yield reasonably good results. Conversely, in larger networks, the effectiveness of more training data becomes more pronounced as graph space complexity grows exponentially.

Obs.❷ Our TICL benefits from the size of training data samples. As TICL relies on quantitatively assessing conditional dependencies using conditional independence as features, as shown in Figure 7, with the continuous increase in sample size, the independence tests become more stable. Thus, TICL demonstrates improvement across various performance metrics in different graphs.

4.3 Sampling and Running Efficiency (RQ3)

We maintain the basic setup and assess the efficiency of our method from two perspectives.

Sampling Time. Given that the starting point strategy already demonstrates efficient rapid convergence, we evaluate the second multi-chain MCMC strategy by comparing it to the single-chain approach. As shown in Figure 8 (a), compared to the single-chain method, the sampling time consumed by multi-chain MCMC maintains a limited increase as the size of the graph grows, with a significant improvement in acceleration efficiency. This is primarily due to the inherent parallel adaptability of the our IS-MCMC, highlighting the efficiency of the multi-chain strategy.

Running Time. We further compare the execution and inference times of all baseline methods. As shown in Figure 8 (b), we record the time intervals consumed by different methods, leading to two observations: ❶ **Inefficiency of other learning-based methods**. These methods typically require around 100-500 seconds of runtime, whereas most non-SCL methods complete tasks within 50 seconds. This discrepancy is mainly due to the slow nature of gradient optimization. ❷ **Our method achieves efficiency similar to non-SCL methods.** Moreover, although our training time may include proxy algorithms, this is not mandatory, as the random seed is optional. Therefore, it depends on the actual scenario; if dealing with causal discovery in high-risk areas, time cost becomes a secondary consideration.

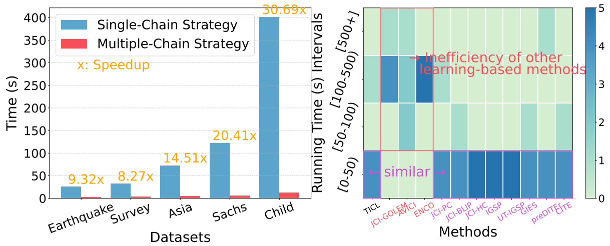

(a) Sampling Time Study

(b) Running Time Study

Figure 8: Efficiency study.

4.4 Different Intervention Settings Study (RQ4)

We further conducted experiments and analyses on **RQ4** regarding intervention types, intervention ratios, and test sample sizes. Due to the complex diversity of different situations, this has been rarely considered comprehensively before. Nevertheless, our results still demonstrate the consistent superiority of TICL across various settings. Due to page limitation, more analysis see Appendix F.

5 Conclusion

In conclusion, TICL offers a novel solution to the problem of causal discovery from interventional data, particularly in the face of distribution shifts between training and test data. TICL employs the *test-time training*, namely, accessing test data and using self-augmentation through the IS-MCMC process to obtain training data. By introducing this technique that generates training data at test time, TICL adapts to the biases inherent in the test distribution, thereby bypassing domain generalization issues. Our approach to training data acquisition highlights a novel application of posterior estimation: leveraging epistemic uncertainty to generate high-quality test-time training data. This method enhances model performance and underscores its potential in advancing SCL. Our integration of the JCI framework with SCL, through a learning-based modification of the PC algorithm, enables more effective causal inference from self-augmented training data. The extensive experimental results demonstrate that TICL outperforms existing methods in both causal structure inference and interventional target detection, underscoring its robustness and adaptability in real-world scenarios.

REFERENCES

Alan Agresti. Categorical data analysis, volume 792. John Wiley & Sons, 2012.

Réka Albert and Albert-László Barabási. Statistical mechanics of complex networks. Reviews of modern physics, 74(1):47, 2002.

Yashas Annadani, Nick Pawlowski, Joel Jennings, Stefan Bauer, Cheng Zhang, and Wenbo Gong. Bayesdag: Gradient-based posterior inference for causal discovery. Advances in Neural Information Processing Systems, 36:1738–1763, 2023.

Philippe Brouillard, Sébastien Lachapelle, Alexandre Lacoste, Simon Lacoste-Julien, and Alexandre Drouin. Differentiable causal discovery from interventional data. Advances in Neural Information Processing Systems, 33:21865–21877, 2020.

Tianqi Chen and Carlos Guestrin. Xgboost: A scalable tree boosting system. In Proceedings of the 22nd acm sigkdd international conference on knowledge discovery and data mining, pp. 785–794, 2016.

J Cheng, R Greiner, J Kelly, D Bell, and W Liu. Learning bayesian networks from data: An information-theory based approach department of computing sciences. Artificial intelligence, 137: 43–90, 2002.

David Maxwell Chickering. Learning equivalence classes of bayesian-network structures. The Journal of Machine Learning Research, 2:445–498, 2002a.

David Maxwell Chickering. Optimal structure identification with greedy search. Journal of machine learning research, 3(Nov):507–554, 2002b.

Diego Colombo, Marloes H Maathuis, et al. Order-independent constraint-based causal structure learning. J. Mach. Learn. Res., 15(1):3741–3782, 2014.

Pierre Comon. Independent component analysis, a new concept? Signal processing, 36(3):287–314, 1994.

Thomas M Cover. Elements of information theory. John Wiley & Sons, 1999.

James Cussens. Bayesian network learning with cutting planes. arXiv preprint arXiv:1202.3713, 2012.

Haoyue Dai, Rui Ding, Yuanyuan Jiang, Shi Han, and Dongmei Zhang. Ml4c: Seeing causality through latent vicinity. In Proceedings of the 2023 SIAM International Conference on Data Mining (SDM), pp. 226–234. SIAM, 2023.

Payam Dibaeinia and Saurabh Sinha. Sergio: a single-cell expression simulator guided by gene regulatory networks. Cell systems, 11(3):252–271, 2020.

Rui Ding, Yanzhi Liu, Jingjing Tian, Zhouyu Fu, Shi Han, and Dongmei Zhang. Reliable and efficient anytime skeleton learning. In Proceedings of the AAAI Conference on Artificial Intelligence, volume 34, pp. 10101–10109, 2020.

Daniel Eaton and Kevin Murphy. Belief net structure learning from uncertain interventions. J Mach Learn Res, 1:1–48, 2007a.

Daniel Eaton and Kevin Murphy. Exact bayesian structure learning from uncertain interventions. In Artificial intelligence and statistics, pp. 107–114. PMLR, 2007b.

Paul Erdős, Alfréd Rényi, et al. On the evolution of random graphs. Publ. math. inst. hung. acad. sci, 5(1):17–60, 1960.

Ronald Aylmer Fisher, Ronald Aylmer Fisher, Statistiker Genetiker, Ronald Aylmer Fisher, Statistician Genetician, Great Britain, Ronald Aylmer Fisher, and Statisticien Généticien. The design of experiments, volume 21. Oliver and Boyd Edinburgh, 1966.

Arthur Gretton, Kenji Fukumizu, Choon Teo, Le Song, Bernhard Schölkopf, and Alex Smola. A kernel statistical test of independence. Advances in neural information processing systems, 20, 2007.

Wiebke Günther, Urmi Ninad, Jonas Wahl, and Jakob Runge. Conditional independence testing with heteroskedastic data and applications to causal discovery. Advances in Neural Information Processing Systems, 35:16191–16202, 2022.

Alexander Hägele, Jonas Rothfuss, Lars Lorch, Vignesh Ram Somnath, Bernhard Schölkopf, and Andreas Krause. Bacadi: Bayesian causal discovery with unknown interventions. In International Conference on Artificial Intelligence and Statistics, pp. 1411–1436. PMLR, 2023.

Alain Hauser and Peter Bühlmann. Characterization and greedy learning of interventional markov equivalence classes of directed acyclic graphs. The Journal of Machine Learning Research, 13(1): 2409–2464, 2012.

Steven M Hill, Chris J Oates, Duncan A Blythe, and Sach Mukherjee. Causal learning via manifold regularization. 2019.

Patrik Hoyer, Dominik Janzing, Joris M Mooij, Jonas Peters, and Bernhard Schölkopf. Nonlinear causal discovery with additive noise models. Advances in neural information processing systems, 21, 2008.

Markus Kalisch and Peter Bühlman. Estimating high-dimensional directed acyclic graphs with the pc-algorithm. Journal of Machine Learning Research, 8(3), 2007.

Nan Rosemary Ke, Olexa Bilaniuk, Anirudh Goyal, Stefan Bauer, Hugo Larochelle, Bernhard Schölkopf, Michael C Mozer, Chris Pal, and Yoshua Bengio. Learning neural causal models from unknown interventions. arXiv preprint arXiv:1910.01075, 2019.

Nan Rosemary Ke, Olexa Bilaniuk, Anirudh Goyal, Stefan Bauer, Hugo Larochelle, Bernhard Schölkopf, Michael Curtis Mozer, Christopher Pal, and Yoshua Bengio. Neural causal structure discovery from interventions. Transactions on Machine Learning Research, 2023a.

Nan Rosemary Ke, Silvia Chiappa, Jane Wang, Anirudh Goyal, Jorg Bornschein, Melanie Rey, Theophane Weber, Matthew Botvinic, Michael Mozer, and Danilo Jimenez Rezende. Learning to induce causal structure. The Eleventh International Conference on Learning Representations, 2023b.

Daphne Koller and Nir Friedman. Probabilistic graphical models: principles and techniques. MIT press, 2009.

Jack Kuipers and Giusi Moffa. Partition mcmc for inference on acyclic digraphs. Journal of the American Statistical Association, 112(517):282–299, 2017.

Adam Li, Amin Jaber, and Elias Bareinboim. Causal discovery from observational and interventional data across multiple environments. In Thirty-seventh Conference on Neural Information Processing Systems, 2023.

Hebi Li, Qi Xiao, and Jin Tian. Supervised whole dag causal discovery. arXiv preprint arXiv:2006.04697, 2020.

Phillip Lippe, Taco Cohen, and Efstratios Gavves. Efficient neural causal discovery without acyclicity constraints. The Tenth International Conference on Learning Representations, 2022.

Yuejiang Liu, Parth Kothari, Bastien Van Delft, Baptiste Bellot-Gurlet, Taylor Mordan, and Alexandre Alahi. Ttt++: When does self-supervised test-time training fail or thrive? Advances in Neural Information Processing Systems, 34:21808–21820, 2021.

David Lopez-Paz, Krikamol Muandet, and Benjamin Recht. The randomized causation coefficient. J. Mach. Learn. Res., 16:2901–2907, 2015.

Lars Lorch, Scott Sussex, Jonas Rothfuss, Andreas Krause, and Bernhard Schölkopf. Amortized inference for causal structure learning. Advances in Neural Information Processing Systems, 35, 2022.

Pingchuan Ma, Rui Ding, Haoyue Dai, Yuanyuan Jiang, Shuai Wang, Shi Han, and Dongmei Zhang. Ml4s: Learning causal skeleton from vicinal graphs. In Proceedings of the 28th ACM SIGKDD Conference on Knowledge Discovery and Data Mining, pp. 1213–1223, 2022.

David Madigan, Jeremy York, and Denis Allard. Bayesian graphical models for discrete data. International Statistical Review/Revue Internationale de Statistique, pp. 215–232, 1995.

Hakim Manghwar, Bo Li, Xiao Ding, Amjad Hussain, Keith Lindsey, Xianlong Zhang, and Shuangxia Jin. Crispr/cas systems in genome editing: methodologies and tools for sgrna design, off-target evaluation, and strategies to mitigate off-target effects. Advanced science, 7(6):1902312, 2020.

Alessandro Mascaro and Federico Castelletti. Bayesian causal discovery from unknown general interventions. arXiv preprint arXiv:2312.00509, 2023.

Christopher Meek. Causal inference and causal explanation with background knowledge. In Proceedings of the Eleventh conference on Uncertainty in artificial intelligence, pp. 403—410, 1995.

Thomas Minka. Estimating a dirichlet distribution, 2000.

Joris M Mooij, Sara Magliacane, and Tom Claassen. Joint causal inference from multiple contexts. The Journal of Machine Learning Research, 21(1):3919–4026, 2020.

In Jae Myung. Tutorial on maximum likelihood estimation. Journal of mathematical Psychology, 47 (1):90–100, 2003.

Ignavier Ng, Shengyu Zhu, Zhitang Chen, and Zhuangyan Fang. A graph autoencoder approach to causal structure learning. arXiv preprint arXiv:1911.07420, 2019.

Ignavier Ng, AmirEmad Ghassami, and Kun Zhang. On the role of sparsity and dag constraints for learning linear dags. Advances in Neural Information Processing Systems, 33:17943–17954, 2020.

Judea Pearl. Causality. Cambridge university press, 2009.

Jonas Peters and Peter Bühlmann. Structural intervention distance for evaluating causal graphs. Neural computation, 27(3):771–799, 2015.

Anne Helby Petersen, Joseph Ramsey, Claus Thorn Ekstrøm, and Peter Spirtes. Causal discovery for observational sciences using supervised machine learning. arXiv preprint arXiv:2202.12813, 2022.

Joseph Ramsey, Jiji Zhang, and Peter L Spirtes. Adjacency-faithfulness and conservative causal inference. arXiv preprint arXiv:1206.6843, 2012.

Mauro Scanagatta, Cassio P de Campos, Giorgio Corani, and Marco Zaffalon. Learning bayesian networks with thousands of variables. Advances in neural information processing systems, 28, 2015.

Marco Scutari. Learning bayesian networks with the bnlearn r package. Journal of Statistical Software, 2010.

Alex Smola, Arthur Gretton, Le Song, and Bernhard Schölkopf. A hilbert space embedding for distributions. In International conference on algorithmic learning theory, pp. 13–31. Springer, 2007.

Peter Spirtes and Clark Glymour. An algorithm for fast recovery of sparse causal graphs. Social science computer review, 9(1):62–72, 1991.

Peter Spirtes, Clark N Glymour, and Richard Scheines. Causation, prediction, and search. MIT press, 2000.

Chandler Squires, Yuhao Wang, and Caroline Uhler. Permutation-based causal structure learning with unknown intervention targets. In Conference on Uncertainty in Artificial Intelligence, pp. 1039–1048. PMLR, 2020.

Chengwei Su and Mark E Borsuk. Improving structure mcmc for bayesian networks through markov blanket resampling. The Journal of Machine Learning Research, 17(1):4042–4061, 2016.

Yu Sun, Xiaolong Wang, Zhuang Liu, John Miller, Alexei Efros, and Moritz Hardt. Test-time training with self-supervision for generalization under distribution shifts. In International conference on machine learning, pp. 9229–9248. PMLR, 2020.

Jin Tian and Judea Pearl. Causal discovery from changes. In Proceedings of the Seventeenth conference on Uncertainty in artificial intelligence, pp. 512–521, 2001.

Ioannis Tsamardinos, Laura E Brown, and Constantin F Aliferis. The max-min hill-climbing bayesian network structure learning algorithm. Machine learning, 65:31–78, 2006.

Burak Varici, Karthikeyan Shanmugam, Prasanna Sattigeri, and Ali Tajer. Scalable intervention target estimation in linear models. Advances in Neural Information Processing Systems, 34:1494–1505, 2021.

Burak Varici, Karthikeyan Shanmugam, Prasanna Sattigeri, and Ali Tajer. Intervention target estimation in the presence of latent variables. In Uncertainty in Artificial Intelligence, pp. 2013–2023. PMLR, 2022.

Thomas Verma and Judea Pearl. Equivalence and synthesis of causal models. In Proceedings of the Sixth Annual Conference on Uncertainty in Artificial Intelligence, pp. 255–270, 1990.

MK Vijaymeena and K Kavitha. A survey on similarity measures in text mining. Machine Learning and Applications: An International Journal, 3(2):19–28, 2016.

Julius von Kügelgen, Michel Besserve, Liang Wendong, Luigi Gresele, Armin Kekić, Elias Bareinboim, David Blei, and Bernhard Schölkopf. Nonparametric identifiability of causal representations from unknown interventions. Advances in Neural Information Processing Systems, 36, 2024.

Dequan Wang, Evan Shelhamer, Shaoteng Liu, Bruno Olshausen, and Trevor Darrell. Tent: Fully test-time adaptation by entropy minimization. arXiv preprint arXiv:2006.10726, 2020.

Qin Wang, Olga Fink, Luc Van Gool, and Dengxin Dai. Continual test-time domain adaptation. In Proceedings of the IEEE/CVF Conference on Computer Vision and Pattern Recognition, pp. 7201–7211, 2022.

Xiaoqiang Wang, Yali Du, Shengyu Zhu, Liangjun Ke, Zhitang Chen, Jianye Hao, and Jun Wang. Ordering-based causal discovery with reinforcement learning. arXiv preprint arXiv:2105.06631, 2021.

Yuhao Wang, Liam Solus, Karren Yang, and Caroline Uhler. Permutation-based causal inference algorithms with interventions. Advances in Neural Information Processing Systems, 30, 2017.

Jing Xiang and Seyoung Kim. A* lasso for learning a sparse bayesian network structure for continuous variables. Advances in neural information processing systems, 26, 2013.

Karren Yang, Abigail Katcoff, and Caroline Uhler. Characterizing and learning equivalence classes of causal dags under interventions. In International Conference on Machine Learning, pp. 5541–5550. PMLR, 2018.

Yuqin Yang, Saber Salehkaleybar, and Negar Kiyavash. Learning unknown intervention targets in structural causal models from heterogeneous data. In International Conference on Artificial Intelligence and Statistics, pp. 3187–3195. PMLR, 2024.

Tjalling J Ypma. Historical development of the newton–raphson method. SIAM review, 37(4): 531–551, 1995.

Kui Yu, Jiuyong Li, and Lin Liu. A review on algorithms for constraint-based causal discovery. arXiv preprint arXiv:1611.03977, 2016.

Yue Yu, Jie Chen, Tian Gao, and Mo Yu. Dag-gnn: Dag structure learning with graph neural networks. In International Conference on Machine Learning, pp. 7154–7163. PMLR, 2019.

Alessio Zanga, Elif Ozkirimli, and Fabio Stella. A survey on causal discovery: Theory and practice. International Journal of Approximate Reasoning, 151:101–129, 2022.

Jiaqi Zhang, Kristjan Greenewald, Chandler Squires, Akash Srivastava, Karthikeyan Shanmugam, and Caroline Uhler. Identifiability guarantees for causal disentanglement from soft interventions. Advances in Neural Information Processing Systems, 36, 2024.

Xun Zheng, Bryon Aragam, Pradeep K Ravikumar, and Eric P Xing. Dags with no tears: Continuous optimization for structure learning. Advances in neural information processing systems, 31, 2018.

SUPPLEMENTARY MATERIAL

TEST-TIME LEARNING OF CAUSAL STRUCTURE FROM INTERVENTIONAL DATA

TABLE OF CONTENTS

A Background Knowledge and Related Work

A.1 Background Knowledge

In this section, we give basic concepts related to causal graphs and joint causal inference.

A.1.1 Causal Graph-related Conept

Definition A.1 (Directed Acyclic Graph). *A directed acyclic graph (DAG) is a directed graph $\mathcal{G}$ that has no cycles, i.e. no directed paths starting and ending at the same vertex.*

Definition A.2 (Skeleton). *A undirected graph $\mathcal{K} = (V_{\mathcal{K}}, E_{\mathcal{K}})$ represents the skeleton of a causal DAG $\mathcal{G} = (V_{\mathcal{G}}, E_{\mathcal{G}})$ if $(X \to Y) \in E_{\mathcal{G}} \cup (Y \to X) \in E_{\mathcal{G}} \iff (X - Y) \in E_{\mathcal{K}}$.*

Definition A.3 (UT and V-structures). *A triple of variables $\langle X, T, Y\rangle$ in a skeleton is an unshielded triple, or short for UT, if X and Y are adjacent to T but are not adjacent to each other. $\langle X, T, Y\rangle$ can be further oriented to become a v-structure $X \to T \leftarrow Y$, in which T is called the collider.*

Definition A.4 (PC). *Denote the set of parents and children of X in a skeleton as PC_X, in other words, PC_X are the neighbors of X in the skeleton. For convenience, if we discuss PC_X in the context of a UT $\langle X, T, Y\rangle$, we intentionally mean the set of parents and children of X but exclude T. Similarly, PC_T excludes X, Y.*

Definition A.5 (Vicinity). *We define the vicinity of a UT $\langle X, T, Y\rangle$ as $V_{\langle X,T,Y\rangle} := \{X, T, Y\} \cup PC_X \cup PC_Y \cup PC_T$. Vicinity is a generalized version of PC, i.e., the neighbors of $\{X, T, Y\}$ in the skeleton.*

Definition A.6 (Sepsets). *Sepsets $\mathcal{S}$ can be define: $\{\mathcal{S} : X \perp Y | S, S \subset PC_X \cup T,\ or\ S \subset PC_Y \cup T\}$. Under faithfulness assumption, sepsets $\mathcal{S}$ is an ensemble where each item is a subset of variables within the vicinity that d-separates X and Y.*

Definition A.7 (Causal Graph). *A causal graph $\mathcal{G}$ is a graphical description of a system in terms of cause-effect relationships, i.e. the causal mechanism. Specifically, for each edge $(X, Y) \in \mathcal{E}$, X is the direct cause of Y, and Y is the direct effect of X, satisfying the causal edge assumption, i.e., the value assigned to each variable X is completely determined by the function $\mathcal{F}$ given its parent. Formally, this can be expressed as: $X_i := f(Pa(X_i))$, $\forall X_i \in \mathcal{V}$.*

As natural consequence of such definitions, we can define models that entail both the structural representation and the set of functions that regulate the underlying causal mechanism.

Definition A.8 (Structural Causal Model). *A structural causal model (SCM) is defined by the tuple $\mathcal{M} = (\mathcal{V}, \mathcal{U}, \mathcal{F}, P)$, where:*

- *$\mathcal{V}$ is a set of endogenous variables, i.e. observable variables,*
- *$\mathcal{U}$ is a set of exogenous variables, i.e. unobservable variables, where $\mathcal{U} \cup \mathcal{V} = \emptyset$*
- *$\mathcal{F}$ is a set of functions, where each function $f_i \in F$ is defined as $fi := (\mathcal{V} \cup \mathcal{U})^p \to \mathcal{V}$, with p the ariety of f_i, so that f_i determines completely the value of V_i,*
- *P is a joint probability distribution over the exogenous variables $P(\mathcal{U}) = \prod_i P(\mathcal{U}_i)$.*

Assumption 1 (Causally Sufficiency). *The set of variables V is said to be causally sufficient if and only if every cause of any subset of V is contained in V itself.*

Note that, in our setup, due to the *causality sufficiency*, exogenous variables are ignored.

A.1.2 JCI Assumption-related Conept

Assumption 0 ("Joint SCM"). *The data-generating mechanism is described by a simple SCM $\mathcal{M}$ of the form:*

$$\mathcal{M} : \begin{cases} C_k = f_k(\boldsymbol{X}_{\mathrm{PA}_{\mathcal{H}}(k)\cap\mathcal{I}}, \boldsymbol{C}_{\mathrm{PA}_{\mathcal{H}}(k)\cap\mathcal{K}}, \boldsymbol{E}_{\mathrm{PA}_{\mathcal{H}}(k)\cap\mathcal{J}}), & k \in \mathcal{K}, \\ X_i = f_i(\boldsymbol{X}_{\mathrm{PA}_{\mathcal{H}}(i)\cap\mathcal{I}}, \boldsymbol{C}_{\mathrm{PA}_{\mathcal{H}}(i)\cap\mathcal{K}}, \boldsymbol{E}_{\mathrm{PA}_{\mathcal{H}}(i)\cap\mathcal{J}}), & i \in \mathcal{I}, \\ \mathbb{P}(\boldsymbol{E}) = \prod_{j\in\mathcal{J}} \mathbb{P}(E_j), \end{cases} \tag{1}$$

that jointly models the system and the context. Its graph $\mathcal{G}(\mathcal{M})$ has nodes $\mathcal{I} \cup \mathcal{K}$ (corresponding to system variables $\{X_i\}_{i\in\mathcal{I}}$ and context variables $\{C_k\}_{k\in\mathcal{K}}$).

It will always make this assumption in order to facilitate the formulation of JCI, the following three assumptions that we discuss are optional, and their applicability has to be decided based on a case-by-case basis. Typically, when a modeler decides to distinguish a system from its context, the modeler possesses background knowledge that expresses that the context is exogenous to the system:

Assumption 1. *("Exogeneity") No system variable causes any context variable, i.e.,*

$$\forall k \in \mathcal{K}, \forall i \in \mathcal{I}: \quad i \to k \notin \mathcal{G}(\mathcal{M}).$$

Assumption 2. *("Complete randomized context") No context variable is confounded with a system variable, i.e.,*

$$\forall k \in \mathcal{K}, \forall i \in \mathcal{I}: \quad i \leftrightarrow k \notin \mathcal{G}(\mathcal{M}).$$

JCI Assumption 1 is often easily justifiable, but the applicability of JCI Assumption 2 may be less obvious in practice. Then, Assumption 3 is further stated, which can be useful whenever both JCI Assumptions 1 and 2 have been made as well.

Assumption 3. *("Generic context model") The context graph[2] $\mathcal{G}(\mathcal{M})_{\mathcal{K}}$ is of the following special form:*

$$\forall k \neq k' \in \mathcal{K}: \quad k \leftrightarrow k' \in \mathcal{G}(\mathcal{M}) \quad \wedge \quad k \to k' \notin \mathcal{G}(\mathcal{M}).$$

The following key result essentially states that when one is only interested in modeling the causal relations involving the system variables (under JCI Assumptions 1 and 2), one does not need to care about the causal relations between the context variables, as long as one correctly models the context distribution.

Theorem 1. *Assume that JCI Assumptions 0, 1 and 2 hold for SCM $\mathcal{M}$:*

$$\mathcal{M}: \begin{cases} C_k = f_k(\boldsymbol{C}_{\mathrm{PA}_{\mathcal{H}}(k)\cap\mathcal{K}}, \boldsymbol{E}_{\mathrm{PA}_{\mathcal{H}}(k)\cap\mathcal{J}}), & k \in \mathcal{K}, \\ X_i = f_i(\boldsymbol{X}_{\mathrm{PA}_{\mathcal{H}}(i)\cap\mathcal{I}}, \boldsymbol{C}_{\mathrm{PA}_{\mathcal{H}}(i)\cap\mathcal{K}}, \boldsymbol{E}_{\mathrm{PA}_{\mathcal{H}}(i)\cap\mathcal{J}}), & i \in \mathcal{I}, \\ \mathbb{P}(\boldsymbol{E}) = \prod_{j\in\mathcal{J}} \mathbb{P}(E_j), \end{cases}$$

For any other SCM $\tilde{\mathcal{M}}$ satisfying JCI Assumptions 0, 1 and 2 that is the same as $\mathcal{M}$ except that it models the context differently, i.e., of the form

$$\tilde{\mathcal{M}}: \begin{cases} C_k = \tilde{f}_k(\boldsymbol{C}_{\mathrm{PA}_{\tilde{\mathcal{H}}}(k)\cap\mathcal{K}}, \boldsymbol{E}_{\mathrm{PA}_{\tilde{\mathcal{H}}}(k)\cap\tilde{\mathcal{J}}}), & k \in \mathcal{K}, \\ X_i = f_i(\boldsymbol{X}_{\mathrm{PA}_{\mathcal{H}}(i)\cap\mathcal{I}}, \boldsymbol{C}_{\mathrm{PA}_{\mathcal{H}}(i)\cap\mathcal{K}}, \boldsymbol{E}_{\mathrm{PA}_{\mathcal{H}}(i)\cap\mathcal{J}}), & i \in \mathcal{I}, \\ \mathbb{P}(\boldsymbol{E}) = \prod_{j\in\tilde{\mathcal{J}}} \mathbb{P}(E_j), \end{cases}$$

with $\mathcal{J} \subseteq \tilde{\mathcal{J}}$ and $\mathrm{PA}_{\mathcal{H}}(i) = \mathrm{PA}_{\tilde{\mathcal{H}}}(i)$ for all $i \in \mathcal{I}$, we have that

1. *the conditional system graphs coincide: $\mathcal{G}(\mathcal{M})_{(\mathcal{K})} = \mathcal{G}(\tilde{\mathcal{M}})_{(\mathcal{K})}$;*
2. *if $\tilde{\mathcal{M}}$ and $\mathcal{M}$ induce the same context distribution, i.e., $\mathbb{P}_{\mathcal{M}}(\boldsymbol{C}) = \mathbb{P}_{\tilde{\mathcal{M}}}(\boldsymbol{C})$, then for any perfect intervention on the system variables $(I, \boldsymbol{\xi}_I)$ with $I \subseteq \mathcal{I}$ (including the non-intervention $I = \emptyset$), $\tilde{\mathcal{M}}_{(I,\boldsymbol{\xi}_I)}$ is observationally equivalent to $\mathcal{M}_{(I,\boldsymbol{\xi}_I)}$.*
3. *if the context graphs $\mathcal{G}(\tilde{\mathcal{M}})_{\mathcal{K}}$ and $\mathcal{G}(\mathcal{M})_{\mathcal{K}}$ induce the same separations, then also $\mathcal{G}(\tilde{\mathcal{M}})$ and $\mathcal{G}(\mathcal{M})$ induce the same separations (where "separations" can refer to either d-separations or σ-separations).*

The following corollary of Theorem 1 states that JCI Assumption 3 can be made without loss of generality for the purposes of constraint-based causal discovery if the context distribution contains no conditional independences:

Corollary 2. *Assume that JCI Assumptions 0, 1 and 2 hold for SCM $\mathcal{M}$. Then there exists an SCM $\tilde{\mathcal{M}}$ that satisfies JCI Assumptions 0, 1 and 2 and 3, such that*

1. *the conditional system graphs coincide: $\mathcal{G}(\mathcal{M})_{(\mathcal{K})} = \mathcal{G}(\tilde{\mathcal{M}})_{(\mathcal{K})}$;*

[2] Remember that $\mathcal{G}(\mathcal{M})_{\mathcal{K}}$ denotes the subgraph on the context variables $\mathcal{K}$ induced by the causal graph $\mathcal{G}(\mathcal{M})$.

2. *for any perfect intervention on the system variables* $(I, \boldsymbol{\xi}_I)$ *with* $I \subseteq \mathcal{I}$ *(including the non-intervention* $I = \emptyset$*),* $\tilde{\mathcal{M}}_{(I,\boldsymbol{\xi}_I)}$ *is observationally equivalent to* $\mathcal{M}_{(I,\boldsymbol{\xi}_I)}$*;*
3. *if the context distribution* $\mathbb{P}_{\mathcal{M}}(\boldsymbol{C})$ *contains no conditional or marginal independences, then the same* σ*-separations hold in* $\mathcal{G}(\tilde{\mathcal{M}})$ *as in* $\mathcal{G}(\mathcal{M})$*; if in addition, the Directed Global Markov Property holds for* $\mathcal{M}$*, then also the same* d*-separations hold in* $\mathcal{G}(\tilde{\mathcal{M}})$ *as in* $\mathcal{G}(\mathcal{M})$*.*

A.2 Related Work

In this section, we present some of the most relevant work to the key points of this paper.

A.2.1 Interventional Causal Discovery

Recovering the underlying causal structure from observational and interventional data is a fundamental research problem (Spirtes et al., 2000; Pearl, 2009). When only observational data are available, constraint-based methods identify a directed acyclic graph (DAG) consistent with conditional independence constraints. Notable examples include the PC algorithm (Spirtes & Glymour, 1991) and its variants, such as Conservative-PC Ramsey et al. (2012) and PC-stable (Colombo et al., 2014). Score-based methods, including GES (Chickering, 2002a) and hill-climbing (Koller & Friedman, 2009), search for the optimal DAG under a predefined scoring function combined with constraints. Gradient-based methods further extend score-based approaches by transforming discrete searches into continuous equality constraints, such as NOTEARS (Zheng et al., 2018), GAE (Ng et al., 2019), and GraN-DAG (Yu et al., 2019). *However, without specific assumptions, the identifiability of structures solely derived from observational data is theoretically limited.* Some works have extended causal discovery algorithms to intervention settings (Hauser & Bühlmann, 2012; Wang et al., 2017; Yang et al., 2018; Squires et al., 2020; Zhang et al., 2024; von Kügelgen et al., 2024). For example, GIES (Hauser & Bühlmann, 2012) pioneered the case with known hard interventions, while IGSP (Wang et al., 2017; Yang et al., 2018) introduced a greedy sparse ordering method to handle known general interventions. Building on this, UT-IGSP (Squires et al., 2020) partially addresses the scenario of unknown target interventions. However, given the diversity of intervention data types and experimental strategies, these methods still fail to universally address various intervention scenarios, limiting effective causal identification. *In contrast, our approach offers a unified solution for causal discovery from intervention data by leveraging a joint causal inference framework combined with supervised causal learning methods, achieving practical empirical performance.*

A.2.2 Supervised Causal Learning

Supervised Causal Learning (SCL) is an emerging paradigm of causal discovery, and has demonstrated strong empirical performance. The strength of SCL lies in its ability to learn complex classification mechanisms, contrasting with traditional rule-based logics for detecting causal relations. Early SCL work focused on pairwise causal discovery, such as RCC (Lopez-Paz et al., 2015) and MRCL (Hill et al., 2019). Further efforts have shifted toward multivariate causal discovery, with models like DAG-EQ (Li et al., 2020) and SLdisco (Petersen et al., 2022), which apply to linear causal models. ML4C (Dai et al., 2023) and ML4S (Ma et al., 2022) focus on v-structure detection and skeleton learning, respectively. For interventional data, methods such as CSIvA (Ke et al., 2023b) and AVICI (Lorch et al., 2022) extended SCL to handle known, hard interventions. However, these models are limited in generalization. *In contrast, our approach adopts a test-time training paradigm, which introduces a process that acquires training data during test time. This allows the model to 'overfit' to the specific biases of the test data, addressing the generalization issue and significantly improving performance in real-world settings.*

A.2.3 Test-Time Training

A body of work (Sun et al., 2020; Wang et al., 2020; 2022; Liu et al., 2021) has explored test-time training paradigm to address the challenge of distribution shift in test data. A common approach is to identify an auxiliary task that aids the model in better adapting to the test data. For instance, TTT (Sun et al., 2020) jointly trains a model for rotation prediction and image classification. TTT++ (Liu et al., 2021) extends this by employing a contrastive learning approach as an auxiliary task for adaptation. In the context of causal discovery, test-time training exhibits distinctive characteristics. Unlike prior works, causal discovery benefits from the ability to *generate test-time training data* in a self-supervised manner. We refer to this approach as *self-augmentation*. This self-augmentation allows test-time training data to capture nuances and biases inherent to the test data, thereby making it well-suited for supservised causal learning. Currently, there is limited work in this area, with the most relevant being ML4S (Ma et al., 2022), which proposes a heuristic for generating vicinal graphs at test time for skeleton learning. *To the best of our knowledge, we are the first to present a systematic approach to test-time adaptation in SCL, and we extend it to a broader context of causal discovery in general interventional settings.*

A.2.4 Joint Causal Inference

Joint Causal Inference (JCI) (Mooij et al., 2020) presents a joint causal inference framework aiming to integrate multiple observed outcomes collected during different experiments (*i.e.*, contexts). In this framework, the observed variable set is divided into two disjoint sets: system variables and context variables. After that, S-FCI (Li et al., 2023) builds upon JCI by introducing a new constraint-based algorithm, enabling learning from observational and intervention data across multiple domains. (Mascaro & Castelletti, 2023) also provides a graphical representation theory of I-MEC under general interventions and designs compatible priors for Bayesian inference to ensure score equivalence of indistinguishable structures. Although JCI provides a novel framework for addressing intervention problems and simplifies the unification of different intervention settings for supervised causal learning, it does not directly address the critical questions of what the appropriate learning objectives are when applying supervised learning, and how the learning process should be designed. *To this end, we highlight the overlooked connection between identifiability in ICD and SCL. Through the modified PC-like SCL algorithm, a two-phase learning method is developed for predicting identifiable causal structures ($\mathcal{I}$-CPDAG) while ensuring theoretical identifiability.*

B Inplementation Details

B.1 Test-Time Training Data Acquisition via Self-Augmentation

B.1.1 Parameter Re-Estimation for CPT

The joint distribution represented by a randomly generated conditional probability table (CPT) may significantly differ from the true joint distribution corresponding to the augmented data, thus undermining the forward-sampling process. Therefore, we propose approximating the joint posterior not only on the structure of the causal graph but also on the parameters of its conditional probability distributions. This approach ensures that the distribution of the augmented graph maintains in-domain ”similarity” with the true underlying distribution.

Specifically, we first use maximum likelihood estimation (Myung, 2003) to estimate the conditional probability tables (CPTs) of the initial seed graph. Secondly, during the `IS-MCMC` iteration process, we propose that the CPTs of the current step's graph are determined by the CPTs from the previous step. For each node in the current step's graph, if its parent nodes remain the same as those in the corresponding node from the previous step's graph, its CPT is directly inherited from the previous step. Otherwise, nodes may lose previous parent nodes due to edge deletion or gain new parent nodes due to edge addition as a result of graph structure transformation operations.

For edge deletions that result in the loss of previous parent nodes, we can adjust the CPT by *marginalization*. For instance, in step $t-1$, if node X has parent nodes Y and Z, the corresponding CPT encodes the distribution $P(X|Y,Z)$. In step t, if the edge $Y \to X$ is deleted, the new conditional distribution should encode $P(X|Z)$. This can be naturally achieved by marginalizing out the node Y using the law of total probability, *i.e.*, $P(X|Z) = \sum_y P(X|Z, Y = y)$.

For edge additions that result in new parent nodes, the situation becomes more complicated. For instance, in step t, if a new edge $U \to X$ is added, introducing a new parent node U, the corresponding conditional probability distribution should encode $P(X|Y,Z,U)$. Considering we primarily deal with discrete data, and the *Dirichlet-multinomial* distribution is a natural choice for modeling categorical distributions, we use the Dirichlet distribution to sample different CPTs. Specifically, for each conditional probability distribution $P(X|Y = y, Z = z, U = u)$, we estimate its parameters α_i by maximizing the log-likelihood function of the data, which is given by:

$$
\begin{aligned}
F(\alpha) = \log p(D|\alpha) = \quad & \log \prod_i p(\mathbf{p}_i|\alpha) = \quad \log \prod_i \frac{\Gamma\left(\sum_k \alpha_k\right)}{\prod_k \Gamma(\alpha_k)} \prod_k p_{ik}^{\alpha_k - 1} \\
= \quad & N \left(\log \Gamma \left(\sum_k \alpha_k \right) - \sum_k \log \Gamma\left(\alpha_k\right) + \sum_k (\alpha_k - 1) \log \hat{p}_k \right),
\end{aligned}
$$

where $\log \hat{p}_k = \frac{1}{N} \sum_i \log p_{ik}$ represents the observed sufficient statistics, $\Gamma(x)$ denotes the Gamma function and is defined to be: $\int_0^\infty t^{x-1} e^{-t} dt$. Since this function does not have a closed-form solution, we employ a fixed-point iteration technique (Minka, 2000) to estimate the parameters. The core idea is to find an initial guess for α and iteratively refine it to converge to the maximum likelihood estimate. It seek a function $F(\cdot)$ that provides a lower bound for the log-likelihood function:

$$
F(\alpha) \geq N \left(\left(\sum_k \alpha_k \right) \Psi \left(\sum_k \alpha_k^{old} \right) - \sum_k \log \Gamma(\alpha_k) + \sum_k \alpha_k \log \hat{p}_k + C \right),
$$

where C is a constant dependent on α, ensuring that the function is optimized at α. By setting the gradient to zero, a new iterative value for α is derived:

$$
\alpha_k^i = \Psi^{-1} \left(\Psi \left(\sum_k \alpha_k^{i-1} \right) + \log \hat{p}_k \right),
$$

where inverse digamma function Ψ^{-1} can be efficiently solved using the Newton-Raphson method (Ypma, 1995). Subsequently, for each possible value x of the variable X, we sample from *Dirichlet*$(\beta \alpha_i)$ to obtain $P(X|Y = y, Z = z, U = u)$, thereby forming our target distribution $P(X|Y, Z, U)$. Here, β is a hyperparameter that adjusts the variance, set to 0.25.

B.1.2 Interventional Structural-Markov Chain Monte Carlo

Algorithm 2 Standard IS-MCMC Algorithm

```
Input:
    Chain Length: $T$,    Expected Training Sample Size: $N$
Output:
    Synthetic training data set: $\{(\mathcal{G}^{(1)}, \mathcal{D}^{(1)}), (\mathcal{G}^{(2)}, \mathcal{D}^{(2)}), \ldots\}, (\mathcal{G}^{(N)}, \mathcal{D}^{(N)})$
Pipeline:
    1. Initialize Seed Graph $\mathcal{G}^{(0)} \sim \mathcal{G}_{\mathcal{I}}$
    2. Estimating CPT parameters by maximum likelihood $\Theta^{(0)} = \text{MLE}(\mathcal{G}^{(0)}, \mathcal{D}_{\mathcal{I}})$
    3. for iteration $t = 1, 2, \ldots$ do:
        (a) Propose: $\mathcal{G}^{cand} \sim q(\mathcal{G}^{(t)} \mid \mathcal{G}^{(t-1)})$ with Intervention Constraint.
        (b) Parameter estimate for current graph: $\Theta^{cand} = \text{Estimation}(\mathcal{G}^{cand}, \mathcal{D}_{\mathcal{I}})$
        (c) Calculate Acceptance Probability:$\alpha(\mathcal{G}^{cand} \mid \mathcal{G}^{(t-1)}) = \min\left\{1, \frac{q(\mathcal{G}^{(t-1)}|\mathcal{G}^{cand})P(\mathcal{G}^{cand}|\mathcal{D}_{\mathcal{I}})}{q(\mathcal{G}^{cand}|\mathcal{G}^{(t-1)})P(\mathcal{G}^{(t-1)}|\mathcal{D}_{\mathcal{I}})}\right\}$
        (d) Randomly Sample: $u \sim \text{Uniform}[0, 1]$
        (e) Accept the proposal: $\mathcal{G}^{(t)} \leftarrow \mathcal{G}^{cand}$, if $u < \alpha$ then Reject the proposal: $\mathcal{G}^{(t)} \leftarrow \mathcal{G}^{t-1}$, $\Theta^{(t)} \leftarrow \Theta^{(t-1)}$
        (f) Forward Sampling data: $\mathcal{D}^{(t)} \leftarrow \text{Sampling}(\mathcal{G}^{(t)}, \Theta^{(t)})$
```

We first present the standard version of the IS-MCMC algorithm, as outlined in Algorithm 2. The first step involves initializing the seed graph, which is typically sampled from the prior distribution of the augmented graph. The second step estimates the parameters of the conditional probability tables using maximum likelihood estimation based on the initial graph structure and the augmented data. The main loop of the algorithm consists of three parts: (1) generating a proposed (or candidate) sample graph from the proposal distribution with intervention constraint; (2) calculating the acceptance probability using the acceptance function $\alpha(\cdot)$, based on the proposal distribution and the posterior probability; (3) accepting the candidate sample with probability α (the acceptance probability), or rejecting the candidate sample with probability $1-\alpha$.

Algorithm 3 Fast IS-MCMC Algorithm

```
Input:
    Chain Length: $L$,    Expected Training Sample Size: $N$
Output:
    Synthetic training data set: $\{(\mathcal{G}^{(1)}, \mathcal{D}^{(1)}), (\mathcal{G}^{(2)}, \mathcal{D}^{(2)}), \ldots\}, (\mathcal{G}^{(N)}, \mathcal{D}^{(N)})$
Pipeline:
    1. Initialize Seed Graph with Proxy Algorithm $\mathcal{G}^{(0)} \leftarrow \text{proxy}(\mathcal{D}_{\mathcal{I}})$
    2. Estimating CPT parameters by maximum likelihood $\Theta^{(0)} = \text{MLE}(\mathcal{G}^{(0)}, \mathcal{D}_{\mathcal{I}})$
    3. Parallel $i \in 1, 2, \ldots, N$ do:
        (a) $\mathcal{G}_{(0)} \leftarrow \mathcal{G}^{(t-1)}$
            for iteration $j = 1, 2, \ldots, L$ do: $\mathcal{G}_j \leftarrow$ Mutation Operation with Constraint$(\mathcal{G}_{(j-1)})$
            $\mathcal{G}^{(cand)} \leftarrow \mathcal{G}_{(L)}$
        (b) Reparameterize according to Sec B.1.1: $\Theta^{cand} = \text{Estimation}(\mathcal{G}^{cand}, \Theta^{(t-1)})$
        (c) Calculate Acceptance Probability:$\alpha(\mathcal{G}^{cand} \mid \mathcal{G}^{(t-1)}) = \min\left\{1, \frac{q(\mathcal{G}^{(t-1)}|\mathcal{G}^{cand})P(\mathcal{G}^{cand}|\mathcal{D}_{\mathcal{I}})}{q(\mathcal{G}^{cand}|\mathcal{G}^{(t-1)})P(\mathcal{G}^{(t-1)}|\mathcal{D}_{\mathcal{I}})}\right\}$
        (d) Randomly Sample: $u \sim \text{Uniform}[0,1]$
        (e) Accept the proposal: $\mathcal{G}^{(t)} \leftarrow \mathcal{G}^{cand}$, if $u < \alpha$ then Reject the proposal: $\mathcal{G}^{(t)} \leftarrow \mathcal{G}^{t-1}$,
            $\Theta^{(t)} \leftarrow \Theta^{(t-1)}$
        (f) Forward Sampling data: $\mathcal{D}^{(t)} \leftarrow \text{Sampling}(\mathcal{G}^{(t)}, \Theta^{(t)})$
```

However, as the number of nodes increases, the computational efficiency of the standard IS-MCMC algorithm becomes untenable. Therefore, for the IS-MCMC algorithm applied to large graphs, we enhance it from two aspects. For the initial random seed graph in the first step, we recommend using proxy algorithms such as JCI+BLIP, which can provide a good starting point that is closer to the target graph structure, thereby accelerating the convergence rate. For the iterative MCMC process in the second step, we suggest parallelizing the computation by simultaneously executing multiple chains. Each chain performs consecutive edge perturbations, followed by sequential accept-reject sampling, to conduct approximate computations. The fast IS-MCMC workflow is shown in Algorithm 3. If not specified otherwise, we use the fast IS-MCMC method as the default setting.

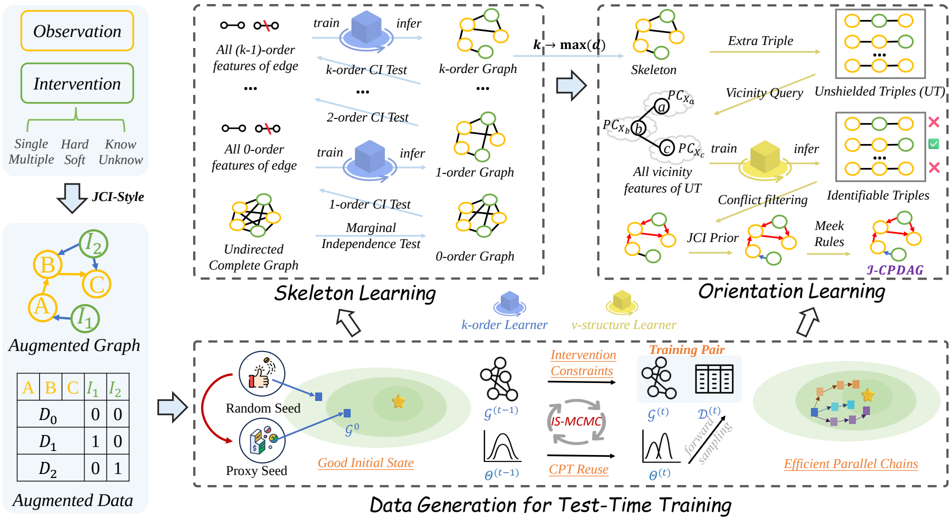

Figure 9: The detailed framework of TICL.

B.2 Two-phase PC-like Supervised Causal Learning

The two-phase supervised learning approach of `TICL` is inspired by the PC algorithm (Spirtes & Glymour, 1991). We first describe the PC algorithm in detail and then reinterpret it from a machine learning perspective, providing a formalization. We also provide detailed feature engineering and techniques. As shown in Figure 9, we further present a more detailed framework diagram, which includes the specific process of two-phase learning.

B.2.1 Revisiting the PC Algorithm

The PC algorithm consists of three main phases, as shown in Algorithm 4. Phase 1 identifies the skeleton and the separating sets, determining the existence of edges. Phase 2 orients the unshielded triples in the skeleton based on the separating sets, establishing edge directionality. Finally, phase 3 further refines the edge directionality using heuristic Meek Rules.

Algorithm 4 Pipeline of `PC` Algorithm Spirtes & Glymour (1991)

```
Require:
    Conditional Independence Information CI among Variables.
    Undirected Complete Graph $\mathcal{C}$ Obtained by Variables.
Output:
    Separation Sets: $\mathcal{SS}$ (Temporary Product)
    Skeleton: $\mathcal{K}$ (Intermediate Product)
    Unshielded Triple Sets of Skeleton: $\mathcal{U}$ (Temporary Product)
    Partially Directed Acyclic Graph, i.e., PDAG: $\mathcal{P}$ (Intermediate Product)
    Completed Partially Directed Acyclic Graph, i.e., CPDAG: $\mathcal{G}$
Pipeline:
    1. Adjacency Determination: Find the skeleton $\mathcal{K}$ and separation sets $\mathcal{SS}$ based on undirected
       complete graph $\mathcal{C}$ and conditional independence information CI using Algorithm 5.
    2. Orientation Determination: Orient unshielded triples $\mathcal{U}$ in the skeleton $\mathcal{K}$ to derive partially
       directed acyclic graph $\mathcal{P}$ based on the separation sets $\mathcal{SS}$ using Algorithm 6.
    3. In $\mathcal{P}$ orient as many of the remaining undirected edges as possible by repeated application
       of rules R1-R3 to derive completed partially directed acyclic graph $\mathcal{G}$.
```

In phase 1, we start with a complete undirected graph $\mathcal{C}$. This graph is then sparsified through iterative conditional tests information **CI**, where an edge $X_i - X_j$ is removed if X_i is conditionally independent of X_j given some subset $\mathcal{S}$ of the remaining variables of the current k-order graph. These conditional independence queries proceed in a cascading manner, making the algorithm computationally efficient for high-dimensional sparse graphs since we only need to query conditional independencies up to order $d-1$, where d is the maximal in degree of the underlying DAG. We summarize this process in Algorithm 5.

In phase 2, it aims to identify V-structures. Specifically, it considers all unshielded triples $\mathcal{U}$ in the skeleton $\mathcal{K}$ and orients an unshielded triple (X_a, X_c, X_b) into a V-structure if and only if X_c is not in the separating set of X_a and X_b. We also summarize this process in Algorithm 6.

In phase 3, heuristic meek rules (Meek, 1995) are further applied iteratively to orient as many of the remaining undirected edges as possible. It contains the following three rules:

- **R1**: If $X_a \to X_b - X_c$ exists, change $X_b - X_c$ to $X_b \leftarrow X_c$ (to avoid creating a new V-structure).
- **R2**: If $X_a \to X_b \to X_c$ exists, change $X_a - X_c$ to $X_a \to X_c$ (otherwise a directed cycle is created).

Algorithm 5 Pipeline of Adjacency Determination / Phrase 1 of the PC Algorithm Kalisch & Bühlman (2007)

```
Require:
    Undirected Complete Graph $\mathcal{C}$ Induced by Variables.
    Sequential Order $k$.
Output:
    Skeleton: $\mathcal{K}$
    Separation Sets: $\mathcal{SS}$
Pipeline:
    $k = 1$
    repeat
        for each adjacent pair $(X_i, X_j)$ in $\mathcal{C}$ do
            for each subset $\mathcal{S} \subseteq adj(\mathcal{C}, X_i)\backslash\{X_j\}$ or $adj(\mathcal{C}, X_j)\backslash\{X_i\}$ with $|\mathcal{S}|= k$ do
                if $X_i$ and $X_j$ are conditionally independent given $\mathcal{S}$ then
                    Delete edge $X_i - X_j$ from $\mathcal{C}$
                    Let separation set $\mathcal{SS}_{(X_i,X_j)} = \mathcal{SS}_{(X_j,X_i)} = \mathcal{S}$
                end if
            end for
        end for                                        ▷ This process can be supervised for learning
        $k = k + 1$
    until all adjacent pairs $(X_i, X_j)$ in $\mathcal{C}$ satisfy $|adj(\mathcal{C}, X_i)\backslash\{X_j\}|< k$
```

Algorithm 6 Pipeline of Orientation Determination / Phrase 2 of the PC Algorithm Kalisch & Bühlman (2007)

```
Require:
    Skeleton: $\mathcal{K}$
    Separation Sets: $\mathcal{SS}$
    Unshielded Triple Sets of Skeleton: $\mathcal{U}$
Output:
    Partially Directed Acyclic Graph, i.e., PDAG: $\mathcal{P}$
Pipeline:
    for each non-adjacent pair $(X_a, X_b)$ with common neighbour $X_c$ in $\mathcal{U}$ do
        if $X_c \notin \mathcal{SS}_{(X_a,X_b)}$ then
            Replace $X_a - X_c - X_b$ in $\mathcal{K}$ by $X_a \rightarrow X_c \leftarrow X_b$
        end if
    end for                                            ▷ This process can be supervised for learning
    $\mathcal{P} = \mathcal{S}$
```

- **R3**: If there are $X_a - X_{c1} \rightarrow X_b$, $X_a - X_{c2} \rightarrow X_b$, and X_{c1}, X_{c2} are not adjacent, change $X_a - X_b$ to $X_a \rightarrow X_b$ (otherwise a new v-structure or a directed cycle is created).

B.2.2 Connecting PC and Supervised Machine Learning

In addition to phase 3, phase 1 and 2 can be considered as classification tasks regarding the determination of the presence of edges and the orientation of unshielded triples based on extracted conditionally independent features. We continue below with a detailed explanation.

■ From a machine learning perspective, we formalize phase 1 as follows:

Task: For the current k-oreder graph, classify whether there is an edge between vertices X_i and X_j.

Featurization: Query a subset $\mathcal{S}$ of the current remaining variables of k-oreder graph, and calculate the conditional dependence between X_i and X_j given $\mathcal{S}$:

$$F^{(k)}_{(X_i,X_j)} = \min_{\mathcal{S} \subseteq \mathbf{X} \setminus \{X_i,X_j\}} \{X_i \sim X_j | \mathcal{S}\}$$

Classifier: Train a binary classifier for $(k+1)$-order graph using current k-order features:

$$C^{(k+1)}_{skeleton}(F^{(k)}_{(X_i,X_j)}) := \begin{cases} \quad adjacent & F^{(k)}_{(X_i,X_j)} \neq 0 \\ non-adjacent & F^{(k)}_{(X_i,X_j)} = 0 \end{cases}$$

■ From a machine learning perspective, we formalize phase 2 as follows:

Task: For all unshielded triples $\mathcal{U}$, classify whether each triple $< X_a, X_c, X_b >$ is a v-structure.

Featurization: Query all separating sets $\mathcal{SS}$ satisfying $X_a \perp X_b | \mathcal{SS}$, and calculate the existence Boolean feature:

$$F_{<X_a,X_c,X_b>} = \begin{cases} 1 & X_c \in \mathcal{SS} \\ 0 & X_c \notin \mathcal{SS} \end{cases}$$

Classifier: Train a binary classifier using features:

$$C_{orientation}(F_{<X_a,X_c,X_b>}) := \begin{cases} \quad v\text{-}structure & F_{<X_a,X_c,X_b>} \neq 0 \\ non-v\text{-}structure & F_{<X_a,X_c,X_b>} = 0 \end{cases}$$

Theorem 3. ***(Spirtes and Glymour (Spirtes et al., 2000))*** *Let the distribution of* $\mathbf{X}$ *be faithful to a DAG* $\mathcal{G}$*, and assume that we are given perfect conditional independence information about all pairs of variables* (X_i, X_j) *in* $\mathbf{X}$ *given subsets* $\mathcal{S} \subseteq \mathbf{X} \setminus \{X_i, X_j\}$*. The output of PC algorithm is the CPDAG that represents* $\mathcal{G}$*.*

However, in practical applications, conditional independence tests relying on data estimates can encounter issues like limited sample size, data quality issues, and intricate dependency structures (Günther et al., 2022). Thus, it is advisable to employ more systematic featurization procedures to enhance classification performance in a more effective and robust manner.

B.2.3 Skeleton and Orientation Feature Engineering

In the realm of skeleton learning, drawing upon the experience of (Cheng et al., 2002; Ding et al., 2020; Xiang & Kim, 2013; Ma et al., 2022), we have extracted primary features of the two categories: quantitative k-order conditional dependencies and local structural information. For orientation learning, again relying on the experience of (Vijaymeena & Kavitha, 2016; Zanga et al., 2022; Dai et al., 2023), we have extracted main features of the two categories: quantitative unshielded triplet conditional dependencies and local structural information. The intuition behind it is detailed below.

In skeleton inference, we first look for useful features of the type of conditional test information. Intuitively, for the numerical vectors resulting from the conditional tests performed on the current node pairs, which indicate the conditional dependency between nodes, we consider them as primary features. Additionally, when conducting higher-order conditional tests, if the dependency relationships decrease significantly, it suggests that they may be blocked by new nodes, so this residual conditional

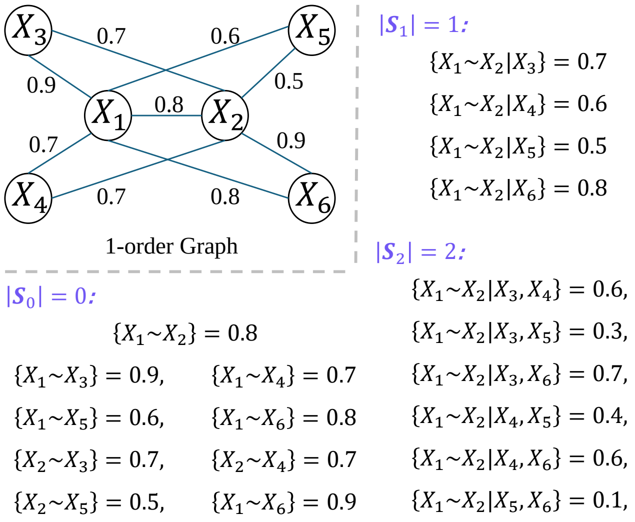
X_3
0.7
0.6
X_5
0.9
0.8
0.5
X_1
X_2
0.7
0.9
X_4
0.7
0.8
X_6
1-order Graph
$|\mathcal{S}_1| = 1$:
$\{X_1 \sim X_2 | X_3\} = 0.7$
$\{X_1 \sim X_2 | X_4\} = 0.6$
$\{X_1 \sim X_2 | X_5\} = 0.5$
$\{X_1 \sim X_2 | X_6\} = 0.8$
$|\mathcal{S}_2| = 2$:
$\{X_1 \sim X_2 | X_3, X_4\} = 0.6,$
$\{X_1 \sim X_2 | X_3, X_5\} = 0.3,$
$\{X_1 \sim X_2 | X_3, X_6\} = 0.7,$
$\{X_1 \sim X_2 | X_4, X_5\} = 0.4,$
$\{X_1 \sim X_2 | X_4, X_6\} = 0.6,$
$\{X_1 \sim X_2 | X_5, X_6\} = 0.1,$
$|\mathcal{S}_0| = 0$:
$\{X_1 \sim X_2\} = 0.8$
$\{X_1 \sim X_3\} = 0.9,$
$\{X_1 \sim X_4\} = 0.7$
$\{X_1 \sim X_5\} = 0.6,$
$\{X_1 \sim X_6\} = 0.8$
$\{X_2 \sim X_3\} = 0.7,$
$\{X_2 \sim X_4\} = 0.7$
$\{X_2 \sim X_5\} = 0.5,$
$\{X_1 \sim X_6\} = 0.9$

Figure 10: Feature extraction example of edge $X_1 - X_2$ in 1-order skeleton graph.

Table 3: The features extracted for skeletal learning. As shown in Figure 10, $k = 2$, is used to illustrate the design intuition and computational examples.

Skeleton Feature				
Type	Name	Calculate	Example Raw Results	Dimension
CI Test Information	k-order Conditional Dependence	$\{X_i \sim X_j \| \mathcal{S}_2\}$, $\|\mathcal{S}_2\| = 2$	[0.6, 0.3, 0.7, 0.4, 0.6, 0.1]	Not Fixed → 15
	Residual Conditional Dependence	$\{X_i \sim X_j \| \mathcal{S}_1\} - \min_{X_q} \{X_i \sim X_j \| \mathcal{S}_2 \cup \{X_q\}\}$, $\|\mathcal{S}_1\| = 1$, $\|\mathcal{S}_2\| = 2$	[0.4, 0.2, 0.4 ,0.7]	Not Fixed → 15
Structural Information	Competitiveness	$\frac{\|\{X_q \| X_q \in nbd(X_i), C_{k-1}(X_i,X_j) > C_{k-1}(X_i,X_q)\}\|}{\|nbd_{\mathcal{G}_{k-1}}(X_i)\| - 1}$, $\frac{\|\{X_q \| X_q \in nbd(X_j), C_{k-1}(X_j,X_i) > C_{k-1}(X_j,X_q)\}\|}{\|nbd_{\mathcal{G}_{k-1}}(X_j)\| - 1}$, $C_{k-1}(X_i, X_j)$	[0.5, 0.75, 0.8]	3
	Degree	$deg(X_i), deg(X_j)$	[4, 4]	2
	Density	$\frac{\|nbd(X_i) \cap nbd(X_j)\|}{\min(\|nbd(X_i)\|, \|nbd(X_j)\|)}$	[1]	1

dependency can be seen as another complementary feature. Considering the structural aspect, conditional independence may be influenced by the information of the local graph structure in which the current node pairs are located. Generally, the sparser the local graph is, the less likely it is to be disconnected by conditional independence tests. Therefore, we select three main features for measurement, including the relative competitiveness of adjacent edges between node pairs, the degrees of node pairs, and the overlapping density of adjacent edges of node pairs. In Figure 10, we provide an example of a 1-order skeleton graph, based on which we further summarize the types of feature variables and calculation methods in Table 3.

In the unshielded triplet orientation, we also seek useful features of the condition test information type. Unlike relying solely on specific triplet condition test information, we extend it to the neighborhood.

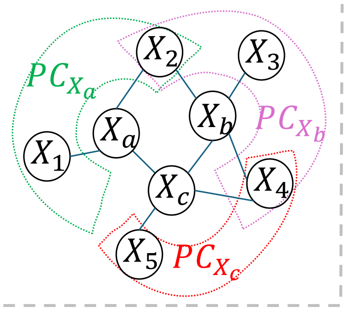

$\{X_a \sim X_b | \emptyset\} = 0.9$ $\{X_a \sim PC_{X_b} | \emptyset\} = 0.7$
$\{X_a \sim X_b | \boldsymbol{SS}\} = 0.8$ $\{X_a \sim PC_{X_b} | \boldsymbol{SS}\} = 0.8$
$\{X_a \sim X_b | X_c\} = 0.8$ $\{X_a \sim PC_{X_b} | X_c\} = 0.8$
$\{X_a \sim X_b | X_c \vee \boldsymbol{SS}\} = 0.6$ $\{X_a \sim PC_{X_b} | X_c \vee \boldsymbol{SS}\} = 0.7$
$\{X_a \sim X_b | PC_{X_c}\} = 0.8$ $\{X_a \sim PC_{X_b} | PC_{X_c}\} = 0.5$
$\{X_a \sim X_b | PC_{X_c} \vee \boldsymbol{SS}\} = 0.7$ $\{X_a \sim PC_{X_b} | PC_{X_c} \vee \boldsymbol{SS}\} = 0.4$
$\{PC_{X_a} \sim X_b | \emptyset\} = 0.8$ $\{PC_{X_a} \sim PC_{X_b} | \emptyset\} = 0.9$
$\{PC_{X_a} \sim X_b | \boldsymbol{SS}\} = 0.4$ $\{PC_{X_a} \sim PC_{X_b} | \boldsymbol{SS}\} = 0.8$
$\{PC_{X_a} \sim X_b | X_c\} = 0.4$ $\{PC_{X_a} \sim PC_{X_b} | X_c\} = 0.9$
$\{PC_{X_a} \sim X_b | X_c \vee \boldsymbol{SS}\} = 0.3$ $\{PC_{X_a} \sim PC_{X_b} | X_c \vee \boldsymbol{SS}\} = 0.7$
$\{PC_{X_a} \sim X_b | PC_{X_c}\} = 0.6$ $\{PC_{X_a} \sim PC_{X_b} | PC_{X_c}\} = 0.6$
$\{PC_{X_a} \sim X_b | PC_{X_c} \vee \boldsymbol{SS}\} = 0.2$ $\{PC_{X_a} \sim PC_{X_b} | PC_{X_c} \vee \boldsymbol{SS}\} = 0.4$

$\boldsymbol{SS} = \{\{X_1\}, \{X_5\}, \{X_1, X_5\}\}$

Variable Domain: $\{X_a \sim X_b,\ X_a \sim PC_{X_b},\ PC_{X_a} \sim X_b,\ PC_{X_a} \sim PC_{X_b}\}$
Condition Domain: $\{\emptyset,\ \boldsymbol{SS},\ X_c,\ X_c \vee \boldsymbol{SS},\ PC_{X_c},\ PC_{X_c} \vee \boldsymbol{SS}\}$

Figure 11: Orientation feature extraction example of unshielded triple $X_a - X_c - X_b$.

Specifically, in addition to testing variables X_a and X_b themselves, we also extend the set variables of their parents and children, PC_{X_a} and PC_{X_b}, as testing variable domains. For the condition variables, in addition to the empty set $\emptyset$, $\mathbf{SS}$, X_c, we further extend the set variables of the parents and children of X_c to the condition domain, including their element-wise union $\mathbf{SS} \vee X_c$, $\mathbf{SS} \vee PC_{X_c}$. Therefore, by selecting a pair of variables from the variable domain and a condition from the condition domain, we obtain a total of $4 \times 6 = 24$ neighborhood conditional dependency features. Furthermore, considering structural information, we overlap numerical and scale numerical measures of the size and overlap features of the sets of the variable domain and the condition domain to reflect the potential sparsity of the local graph structure. As shown in Figure 11, we provide an example of directional feature extraction, based on which we further summarize the types of feature variables and calculation methods in Table 4.

Table 4: The features extracted for orientation learning, as shown in Figure 11, are used to illustrate the design intuition and computational examples.

Orientation Feature				
Type	Name	Calculate	Example Raw Results	Dimension
CI Test Information	Vicinity Conditional Dependence	$\{\text{Variable} \mid \text{Condition}\}$, Variable: $\{X_a \sim X_b, X_a \sim PC_{X_b}, PC_{X_a} \sim X_b, PC_{X_a} \sim PC_{X_b}\}$ Condition: $\{\emptyset, SS, X_c, X_c \vee SS, PC_{X_c}, PC_{X_c} \vee SS\}$	[0.9, 0.8, 0.8, 0.6, 0.8, 0.7, 0.7, 0.8, 0.8, 0.7, 0.5, 0.4, 0.8, 0.4, 0.4, 0.3, 0.6, 0.2, 0.9, 0.8, 0.9, 0.7, 0.6, 0.4]	24
Structural Information	Overlap	$\frac{\lvert set_1 \cap set_1 \rvert}{\min(\lvert set_1 \rvert, \lvert set_2 \rvert)}$, $set \in PC_{X_a}, PC_{X_b}, PC_{X_c}, \mathbf{SS}$, we also add $set_1 = X_c, set_2 = \mathbf{SS}$	[0.5, 0, 0.5, 0.5, 0, 0.5 ,1]	7
	Scaling	$\#PC_{X_a}, \#PC_{X_b}, \#PC_{X_c}$, $\#\mathbf{SS}$, $\frac{1}{\#\mathbf{SS}} \sum_{SS \in \mathbf{SS}} \#SS$	[2, 3, 2, 3, $\frac{4}{3}$]	5

It is noted that the conditional dependence features mentioned above may be dynamically changing, which does not conform to the fixed-size features required by most traditional machine learning models. However, this can be easily addressed through classical kernel mean embedding techniques (Smola et al., 2007) to obtain fixed-length embedding features:

$$\frac{1}{|D|} \sum_{z \in D} (\cos(< w_j, z > + b_j))_{j=1}^{m} \in \mathbb{R}^m.$$

Here, $m = 15$, which signifies that each extended feature now possesses a fresh embedding dimension of 15. Furthermore, we incorporate an extra set of five statistics comprising maximum, minimum, mean, standard deviation, and set size. Consequently, we merge all these derived features to construct the input feature for the model.

Additionally, various methods exist for assessing conditional dependence, such as determining the p-value through testing for conditional independence or using conditional mutual information (Cover, 1999). When dealing with categorical variables, the G2 test is a suitable option (Agresti, 2012). In our approach, we employ an approximate version of the G2 statistic and rely on p-values to evaluate conditional dependence.

It is worth noting that the p-value can become insignificant due to the double-precision bit limit in computers. To overcome this issue, transforming p-values can be employed to mitigate such limitations and offer a means to evaluate conditional dependency. To begin with, we define the complementary error function as:

$$g(z) = 1 - \frac{2}{\sqrt{\pi}} \int_0^z e^{-t^2}\, \mathrm{d}t,$$

and utilize the quantity z as the inverse of g:

$$z = g^{-1}(x).$$

By applying the non-linear transformation of g^{-1} to a given p-value x, we derive a re-scaled quantity that enhances the assessment of conditional dependency. In essence, z can be interpreted as a measure akin to z-scores in a standard normal distribution; for example, if the p-value is 0.01, then $z = 3$, as a value of 3-sigma signifies that the probability of data falling within a 3-sigma range in a normal distribution is 0.99.

C Conevergence of Inteventional Structural-MCMC

In this section, we first confirm the convergence of the posterior distribution in the IS-MCMC algorithm based on the Structure MCMC framework. Furthermore, we provide a detailed discussion of the key factors considered in optimizing the IS-MCMC process.

C.1 Guarantee of Posterior Distribution Convergence

Our IS-MCMC algorithm follows a standardized Structure MCMC process (Madigan et al., 1995; Su & Borsuk, 2016; Kuipers & Moffa, 2017) in the intervention-augmented graph space. Please refer to Algorithm 1, which corresponds to Steps ❶ - ❻ in the main text as a general introduction to the MCMC process.

By employing the Metropolis-Hastings sampler within the standardized Structure MCMC framework, the Markov chain is guaranteed to have a stationary distribution equal to the posterior distribution $P(\mathcal{G} \mid \mathcal{D})$ (Su & Borsuk, 2016).

It is important to note that, under the premise of this theoretical guarantee, the novelty of our work lies in proposing the use of the posterior distribution as the target for acquiring training samples and optimizing feasible solutions in intervention scenarios.

C.2 Optimization Considerations for IS-MCMC

However, two critical factors need to be addressed. First, managing the time complexity of this process is crucial for maintaining efficient inference. Second, ensuring the effectiveness of the IS-MCMC process on the augmented graph.

- **From the TTT-driven perspective on efficiency:** Since we leverage the ”test-time” phase, the convergence speed of MCMC is particularly important. We observed that a good initial state enables the Markov chain to converge faster, as evidenced by Figure 5 in the experimental section of our paper. Additionally, we modified the algorithm to use parallel multi-chain sampling, allowing for more efficient exploration of the graph space, as shown in Figure 8 of our experimental results.

- **From the JCI-driven perspective on adaptability:** The MCMC process operates on augmented graphs rather than standard causal graphs. Thus, additional constraints are required to ensure the validity of the augmented graph. To address this, we introduced intervention constraints to ensure consistency of the augmented graph within the JCI framework.

In summary, our `IS-MCMC` algorithm effectively addresses multiple challenges under the TTT + JCI framework and demonstrates that using posterior estimates as training data is highly beneficial for test-time SCL.

D Identifiability Theory of PC-Like Supervised Causal Learning

D.1 Intuitive Analysis

D.1.1 Observation

We use the observations from phase 2 as an illustration. As mentioned in Section B.2, we formalize the v-structure orientation of PC as a specific classification problem, that is, determining whether the non-shielded triple $\langle X_a, X_c, X_b \rangle$ forms a v-structure by classifier C_{PC}.

The logic of PC's orientation is clearly asymptotically correct (*i.e.*, the **CI** test becomes fully accurate when the number of records goes to infinity). However, in practice, when the number of records is finite, its empirical performance is not satisfactory. Thus, further enhancements, such as *Majority-PC* (MPC) (Colombo et al., 2014), have been developed to address this limitation.

MPC is a sample-based enhancement of PC's orientation, achieving better performance with finite samples. Instead of identifying only one separating set $\mathcal{SS}$, MPC finds all possible separating sets $\mathcal{SS}$ and counts how many of them contain X_c. The logic can be recast as follows:

Featurization: Finds all separating sets $\mathcal{SS}$ of X_a, X_b, and defines a real-valued feature:

$$F_{<X_a, X_c, X_b>} = \frac{|\{S_i | X_c \in S_i \in \mathcal{SS}\}|}{|\mathcal{SS}|}$$

Classifier: Train a binary classifier using features:

$$C_{MPC}(F_{<X_a,X_c,X_b>}) := \begin{cases} v\text{-}structure & F_{<X_a,X_c,X_b>} \leq 0.5 \\ non-v\text{-}structure & F_{<X_a,X_c,X_b>} > 0.5 \end{cases}$$

Theoretically, both PC and MPC, as ”hand-crafted” classifiers, are asymptotically correct. However, in practice, MPC exhibits greater complexity in its classification mechanism compared to PC, resulting in improved empirical performance. Nonetheless, from a machine learning perspective, both PC and MPC remain ”simple” in terms of their feature representation and classification strategies.

D.1.2 Motivation

The primary motivation for modifying PC into a PC-like SCL method is to leverage *both theoretical identifiability and enhanced empirical performance*:

- **Theoretical Guarantees.** Our PC-like SCL approach *retains* the asymptotic properties of the original PC algorithm. Specifically, the method detects the correct CPDAG (or $\mathcal{I}$-CPDAG in the interventional setting) when the sample size approaches infinity. This ensures theoretical identifiability.
- **Empirical Performance.** In finite-sample scenarios, where PC's reliance on conditional independence (CI) tests can lead to errors, the SCL approach outperforms traditional methods. By combining feature-rich representations with a robust classification mechanism, SCL achieves superior empirical results, as demonstrated in our paper, by comparing `TICL` with PC-JCI or other non-SCL methods. Similar empirical evidences are also presented in prior works (Li et al., 2020; Ma et al., 2022; Dai et al., 2023).

D.2 Advantage

Building on these observations and motivation analysis, our goal is to design a PC-like SCL algorithm that maintains theoretical asymptotic correctness while encouraging a more systematic feature representation and enabling the learning of more sophisticated classification mechanisms. This approach aims to make our method more ”robust” than PC, achieving superior empirical performance. Specifically, Our PC-Like SCL method generalizes these ideas:

- **Featurization:** SCL extracts a richer set of features that capture conditional dependencies and structural patterns around $\langle X_a, X_c, X_b \rangle$.
- **Classifier:** Instead of relying on heuristic rules like C_{PC} or C_{MPC} , we train a classifier on synthetic data. The model learns complex interactions among features, avoiding the limitations of error-prone conditional independence (CI) tests.

In the asymptotic regime, the learned classifier converges to an equivalent, theoretically correct solution like C_{PC} or C_{MPC}. However, in practical settings, SCL's broader feature set and data-driven optimization enable significantly better empirical performance. For example, Table 1 and 2 compare JCI+SCL with JCI-PC and other non-SCL methods, clearly showing SCL's superiority.

D.3 Theoretical Analysis

D.3.1 Restating the PC-like SCL Process

The PC-like SCL approach proposed in our paper consists of two phases:

- **Phase 1: Skeleton Learning.** A binary classifier C_1 takes the feature set (as detailed in Table 3 and Figure 10) as input and predicts the existence of edges between all pairs of nodes.
- **Phase 2: Orientation Learning.** A binary classifier C_2 takes the feature set (as detailed in Table 4 and Figure 11) as input and predicts the v-structure for each unshielded triple (UT), using the skeleton learned from Phase 1.

Finally, Meek's rules are applied to orient as many causal directions as possible.

We aim to prove that both C_1 and C_2 are asymptotically correct (*i.e.*, they output results equivalent to those of the PC algorithm when the sample size approaches infinity). For simplicity, we demonstrate the proof for C_2, as the proof for C_1 follows the same principle.

D.3.2 Asymptotic Correctness of the PC-like SCL Approach

Definition D.1 (Overlap Coefficient)**.** $\mathrm{OLP}\left(\mathbf{A}, \mathbf{B}\right) := |\mathbf{A} \cap \mathbf{B}| / \min\left(|\mathbf{A}|, |\mathbf{B}|\right)$*, where* $\mathbf{A}$ *and* $\mathbf{B}$ *are two sets of variables.*

Definition D.2 (Discriminative Predicate)**.** *A discriminative predicate is a binary predicate function defined over the domain of* C_2*'s feature vector. It can be regarded as a special classifier with a predefined mechanism.*

Definition D.3 (Strong Predicate)**.** *A strong discriminative predicate satisfies the following two criteria when applied to a UT's feature vector: (a) It evaluates to* ***’true’*** *if the UT forms a v-structure. (b) It evaluates to* ***’false’*** *if the UT does not form a v-structure.*

A strong predicate is ***asymptotically correct*** because its output aligns with that of the PC algorithm when the sample size approaches infinity. The key statement here is that there exists at least one strong predicate, meaning we can construct a static classifier using the proposed feature set to achieve asymptotic correctness.

Lemma 4 (Existence of a Strong Predicate)**.** *For a canonical dataset with infinite samples, the predicate* $\mathrm{OLP}\left(X_c, \mathcal{S}\right) = 0$ *is a strong discriminative predicate. It corresponds precisely to the v-structure detection logic of the PC algorithm.*

Proof. According to the PC algorithm's asymptotic correctness theorem:

For a canonical dataset with infinite samples (assuming faithfulness and perfect conditional independence information):

- If an unshielded triple $\langle X_a, X_c, X_b \rangle$ forms a v-structure, then X_c does **not** belong to any separation set of (X_a, X_b).
- If $\langle X_a, X_c, X_b \rangle$ does not form a v-structure, then X_c belongs to **all** separation sets of (X_a, X_b).

In this setting (infinite samples), there is no ambiguity: X_c is either in all separation sets or in none of them.

Now consider the predicate OLP $(X_c, \mathcal{S}) = 0$, which evaluates to **true** if and only if $X_c \notin \mathcal{S}$ for all $\mathcal{S} \in \mathcal{SS}$.

- This implies that $\langle X_a, X_c, X_b \rangle$ is a v-structure.
- Therefore, OLP $(X_c, \mathcal{S}) = 0$ is a strong predicate because it perfectly discriminates v-structures from non-v-structures.

□

Theorem 5 (Asymptotic Correctness of C_2)**.** *By employing a learning model with the universal approximation property, the classifier C_2 is asymptotically correct when classifying a canonical dataset with infinite samples.*

Proof. From Lemma 4, there exists a strong discriminative predicate P that achieves zero loss on a canonical dataset with infinite samples.

- Given P as the ground truth for v-structure detection, a machine learning model with universal approximation capability can approximate P to arbitrary precision, achieving performance no worse than P.
- Additionally, there may exist multiple strong predicates that satisfy the criteria of Definition D.3. Therefore, C_2 can converge to any one of these strong predicates in the asymptotic regime.

□

Summary: The theoretical guarantees demonstrate that the PC-like SCL approach, by leveraging the universal approximation capabilities of learning-based classifiers, retains the asymptotic correctness of the original PC algorithm while enabling superior empirical performance on finite data.

E Experimental Details

E.1 Benchmark

Our experiments are carried out on 14 different causal graph datasets inspired by real-world applications from bayesian network repository [3]. All discrete networks undergo thorough quality checks and necessary repairs, ensuring that the sum of all conditional probability distributions is 1, there are no single-level virtual nodes, and there are no dependencies. The statistics of these bayesian networks are shown in Table 5. We also provide visualizations of some causal graphs, as shown in Figure 12.

E.2 Baselines

The development history of causal discovery from interventional data has been a gradual and incremental process. Here is a detailed introduction to some key works in this field:

- **GIES (Hauser & Bühlmann, 2012):** *This paper first extends the concept of Markov equivalence of Directed Acyclic Graphs for the first time to the case of interventional distributions arising from multiple interventional experiments.* It further demonstrates that under reasonable assumptions of interventional experiments, the intervened Markov equivalence defines a more refined DAG partition than the observed Markov equivalence, thereby enhancing the identifiability of causal models. Moreover, they generalize the greedy equivalence search algorithm, proposing a greedy interventional equivalence search algorithm for regularized maximum likelihood estimation under such intervened conditions.

[3] https://www.bnlearn.com/bnrepository/

Table 5: Statistics and description of bayesian networks we used.

Network	#Nodes	#Edges	#Parameters	Max in-degree	Avg. degree
Earthquake	5	4	10	2	1.60
Survey	6	6	21	2	2.00
Asia	8	8	18	2	2.00
Sachs	11	17	178	3	3.09
Child	20	25	230	2	2.50
Insurance	27	52	1,008	3	3.85
Water	32	66	10,083	5	4.12
Mildew	35	46	540,150	3	2.63
Alarm	37	46	509	4	2.49
Barley	48	84	114,005	4	3.50
Hailfinder	56	66	2,656	4	2.36
Hepar2	70	123	1,453	6	3.51
Win95pts	76	112	574	7	2.95
Pathfinder	109	195	72,079	5	3.58

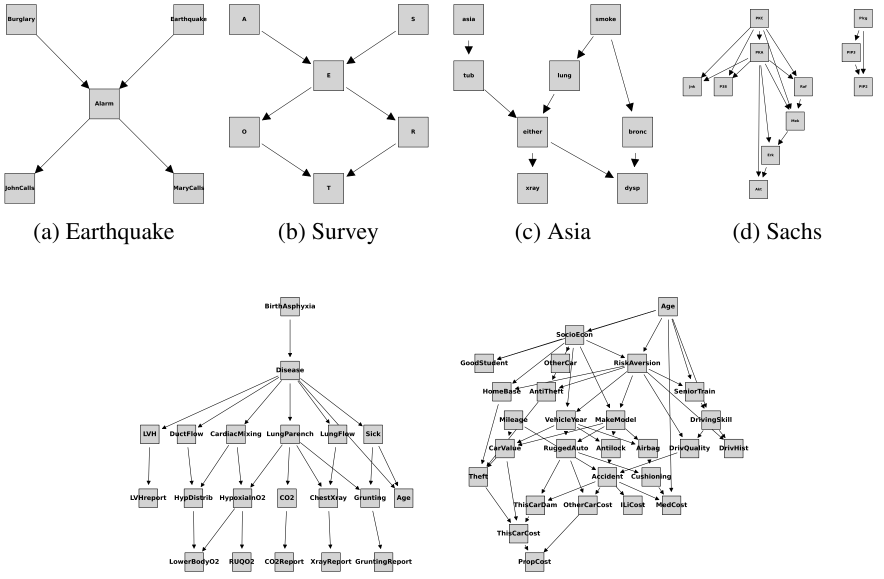

(a) Earthquake (b) Survey (c) Asia (d) Sachs

(e) Child (f) Insurance

Figure 12: Graph Visualizations.

- **IGSP (Wang et al., 2017; Yang et al., 2018):** In this paper, the authors propose two algorithms that utilize both observational and interventional data with consistency guarantees, and prove their consistency under the faithfulness assumption. These algorithms are intervention-adapted versions of the Greedy SP algorithm, and they are non-parametric, which makes them applicable to the analysis of non-Gaussian data as well. Subsequently, *they first extend these identifiability results to general interventions that can modify the dependencies between the target variable and its causes without eliminating them*, and propose the first consistent algorithm for learning a DAG in such an environment.
- **UT-IGSP (Squires et al., 2020):** In this paper, *the authors further extend interventions to unknown scenarios, that is, the problem of estimating causal Directed Acyclic Graph models from a mixture of observational and interventional data when the intervention targets are partially or completely unknown.* They describe the intervened Markov equivalence classes of DAGs that can be identified

from interventional data with unknown intervention targets. Additionally, they propose a provably consistent algorithm for learning the intervened Markov equivalence class from such data. The algorithm greedily searches the permutation space to minimize a novel scoring function. This algorithm is also non-parametric.

- **DCDI (Brouillard et al., 2020):** In this paper, *the authors first introduce a theoretically grounded method for learning causal structures based on neural networks that can utilize interventional data.* They present two instances of this approach: one that relies on normalizing flows as a universal density approximator. They also demonstrate that the precise maximization of the proposed score will identify the $\mathcal{I}$-Markov equivalence classes of causal graphs for both known and unknown target settings.
- **ENCO (Lippe et al., 2022):** In this paper, the authors explore score-based methods for causal discovery from observational and interventional data. They argue that such methods often require constrained optimization to enforce acyclicity or lack convergence guarantees. Consequently, they formulate graph search as an optimization of the likelihood of independent edges, where the direction of edges is modeled as separate parameters. Thus, they provide convergence guarantees when interventions on all variables are available, without the need to constrain the acyclicity of the scoring function.
- **BaCaDI (Hägele et al., 2023):** In this paper, the authors aim to discuss the issue of causal discovery in the realistic scenario where interventional data is scarce. To address this shortcoming, they provide a principled Bayesian approach that operates within the continuous space of causal Bayesian networks (CBNs) and the latent probability representations of interventions. This enables them to approximate complex joint posteriors through efficient, gradient-based particle variational inference techniques, making it applicable to causal systems with many variables.

Recently, Supervised Causal Discovery, which aims to compress data and map between causal relations using pre-synthesized causal graph datasets, has shown impressive performance in test data. We introduce some key works on supervised causal discovery from intervention data:

- **CSIvA (Ke et al., 2023b):** In this paper, the authors believe that meta-learning enables models to generalize well to data from natural causal Bayesian networks, even with relatively few assumptions made during training on synthetic data. *Therefore, they introduce for the first time a supervised approach to tackle the problem of causal structure induction.* This method maps datasets composed of both observational and interventional samples to a structure. By introducing a novel transformer architecture, they aim to discover relations between variables across samples.
- **SDI (Ke et al., 2019; 2023a):** In this paper, the authors introduce a novel neural network-based method for causal discovery from interventional data, capable of handling unknown interventions. By utilizing two sets of distinct parameters to model the causal mechanisms and the structure of the causal graph, experimental evidence indicates that this method can generalize to unseen interventions and can effectively perform partial graph discovery.
- **AVICI (Lorch et al., 2022):** In this work, the authors posit that designing appropriate scores or tests that capture prior knowledge is challenging. Therefore, they propose amortizing the learning of causal structures, which involves training a variational inference model to directly predict causal structures from observational or interventional data. This approach leverages permutation invariance to exhibit robust generalization capabilities, particularly in the challenging field of genomics.

Due to the limitations inherent in the type of methods and the constraints of the assumptions made, they are generally unable to effectively process interventional data across various experimental scenarios. Here, we further summarize, based on the experiments of their paper, the basic setup of their causal discovery from interventional data, as depicted in Table 6:

Most existing intervention dataset learning methods have typically required a known set of intervention targets, which is often a strong assumption. Therefore, when intervention targets are unknown, this naturally poses a challenge: how to identify intervention nodes individually becomes a key issue in structural learning. This task is of practical significance. For instance, in the realm of gene editing, techniques can cleave off-target genomic sites. Evaluating and detecting off-target effects accurately and devising corresponding strategies constitute significant research directions in current gene editing studies (Manghwar et al., 2020). Limited attention has been given to exploring methods for identifying intervention targets. We provide an introduction as follows:

Table 6: Summary of basic settings for various methods of causal discovery from intervention data

Methods	Groun-Truth DAG		Testing Data			Intervention Experiment		
	Type	#Variable	Type	#Obs.	#Int. / per exp.	Type	#Int. Family	#Int. Target
GIES	Random Graph Kalisch & Bühlman (2007) (Linear Gaussian SEM)	10 $\sim$ 50	Continue	50 $\sim$ 10k	50 $\sim$ 10k	Single / Multiple Know Hard	#Var. * {.0 / .2 / .4 / .6 / .8 / 1.0}	1 $\sim$ 4
IGSP	ER (Linear Gaussian SEM)	10 $\sim$ 20	Continue	1k $\sim$ 100k	1k $\sim$ 100k	Single / Multiple Know Hard / Soft	1 $\sim$ 2	#Var. * {0.4 / 0.5}
UT-IGSP	ER (Linear Gaussian SEM)	20	Continue	1k $\sim$ 5k	1 $\sim$ 5k	Single / Multiple Know / Unknow Hard / Soft	Know: (5) + Unknow: (5)	Know: (1) + Unknow: (0 $\sim$ 3)
DCDI	ER (LGM / ANM / NN)	10-20	Continue	10k	10k	Single / Multiple Know / Unknow Hard / Soft	#Variable	#Var. * 0.1
SDI	Random Graph (NN) bnlearn	3 $\sim$ 13	Discrete	2560 (from code)	1111 (from code)	Single Know Soft	#Variable	1
CSIvA	ER (LGM / ANM / NN) (MLP / Dirichlet)	30 $\sim$ 80	Continue	100 $\sim$ 1.5k	100 $\sim$ 1.5k	Single Know / Unknow Hard / Soft	#Variable	1
ENCO	Random Graph (NN) bnlearn	25	Discrete	1k $\sim$ 100k	20 $\sim$ 200	Single Know Soft	#Variable	1
AVICI	ER / SF / WS / SBM / GRG (Linear / Random Fourier)	30	Continue	200 (from code)	20 (from code)	Single Know Hard / Soft	#Var. * .5	1
BaCaDI	ER / SF / SERGIO Dibaeinia & Sinha (2020) (Linear / Nolinear Gaussian)	20	Continue	100	10	Single Know / Unknow Hard / Soft	#Variable	1
TICL	bnlearn	5-109	Discrete	2k $\sim$ 10k	1k $\sim$ 10k	Single / Multiple Know / Unknow Hard / Soft	#Var. * {.0 / .2 / .4 / .8 }	1$\sim$ 3

- **UT-IGSP (Squires et al., 2020):** As mentioned before, the UT-IGSP algorithm learns the intervention targets while learning the causal structure. Although the intervention refines the search space, greedy search of the sparsest permutations is very slow in the case of high-dimensional data, especially when using non-Gaussian conditional independence test.
- **CITE (Varici et al., 2021):** In this paper, the authors primarily address the problem of estimating unknown intervention targets in causal directed acyclic graphs based on observational and interventional data. The focus lies on soft interventions within the framework of linear structural equation models. They propose a scalable and efficient algorithm capable of consistently identifying all intervention targets. The key idea is to estimate the intervention sites based on the difference between precision matrices associated with the observed data set and the intervened data set.
- **PreDITEr (Varici et al., 2022):** After that, the authors of this paper further extend the previous method by eliminating the need to learn the entire causal model, focusing solely on learning intervention targets. The key point is to leverage the sparse changes imposed on the precision matrix of the linear model by intervention measures, composed of a series of precision difference estimation steps. Additionally, they infer the knowledge required to refine observational Markov equivalence classes into interventional MECs.
- **LIT (Yang et al., 2024):** In this paper, the authors tackle for the first time the problem of identifying unknown intervention targets in a multi-environment setting. They further consider cases within the intervention target set that allow for potential confounding factors. They propose a two-stage algorithm to recover exogenous noise and match it with the corresponding endogenous variables. Under the assumption of causal sufficiency, intervention targets can be uniquely identified. In cases where potential confounding factors exist, a candidate intervention target set is provided, offering more information compared to previous works.

As shown in Table 7, we provide a comparison to briefly illustrate the types of unknown intervention experiments supported by the above intervention target detection algorithms.

To ensure fair experimentation, algorithms and hyperparameter tuning are involved in each of our experiments. For all baseline algorithms, we explore critical hyperparameters that govern their interactions, and report the best results. Moreover, we use open source code for all algorithms for evaluation, including code from the authors as well as various popular toolkits. The public code for the baseline is also included at the URL below.

Table 7: Comparison of situations (more suitable) supported by intervention target detection methods.

Methods	**Causal Insufficiency**	**Interv. Frequency**		**Interv. Mechanism**		**Data Type**		**Domain**	
		Single	Multiple	Hard	Soft	Continue	Discrete	Single	Multiple
UT-IGSP	✗	✓	✓	✓	✓	✓	∼	✓	✓
CITE	✗	✓	✓	∼	✓	✓	∼	✓	✗
PreDITEr	✗	✓	✓	∼	✓	✓	∼	✓	✗
LIT	✓	✓	✓	∼	✓	✓	∼	✓	✓

Firstly, we introduce a method specifically designed for causal discovery from observational and interventional data:

- **GIES:** - Score Function: Gaussian BIC, https://github.com/juangamella/gies
- **IGSP:** - Significance $\alpha \in \{1\text{e}3, 1\text{e}4\}$, CI test $\in \{\text{Gaussian}, \text{kci}, \text{hsic}\}$, https://github.com/uhlerlab/graphical_model_learning
- **UT-IGSP:** - Significance $\alpha \in \{1\text{e}3, 1\text{e}4\}$, CI test $\in \{\text{Gaussian}, \text{kci}, \text{hsic}\}$, https://uhlerlab.github.io/causaldag/utigsp.html
- **ENCO:** - Sparsity Regularizer $\lambda_{sparse} \in \{0.002, 0.02\}$, Epochs $\in \{50, 100\}$, https://github.com/phlippe/ENCO
- **AVICI:** - Model $\in \{\text{scm-v0}, \text{linear}, \text{rff}, \text{grn}\}$, https://github.com/larslorch/avici

As mentioned in the main text, joint causal inference offers a robust theoretical framework that effectively combines interventional and observational data, simplifying causal discovery algorithms to operate solely on observational setting. We select four distinct algorithmic combinations, with parameter settings as follows:

- **PC** - variant $\in \{\text{original, stable}\}$, Significance $\alpha \in \{0.05,\ 0.01\}$, CI test $\in \{\text{fisherz}, \text{g2}, \text{chi2}\}$, https://github.com/huawei-noah/trustworthyAI/tree/master/gcastle
- **HC** - Score Function: Bdeu Score, https://github.com/pgmpy/pgmpy
- **BLIP** - Time $\in \{60,\ 300,\ \#\text{Variable}\}$, https://cran.r-project.org/web/packages/r.blip/
- **GOLEM** - $\lambda_1 \in \{2\text{e-}2, 2\text{e-}3\}$, $\omega \in \{0.2, 0.3\}$, https://github.com/ignavierng/golem

Finally, for the specific task of intervention target detection, the configuration parameters for the comparative methods are as follows:

- **CITE** - $\lambda_{l1} \in \{1\text{e-}1, 5\text{e-}1\}$, $\text{Parent}_{l1} \in \{5\text{e-}3, 1\text{e-}2, 2\text{e-}2, 3\text{e-}2, 4\text{e-}2, 5\text{e-}2, 6\text{e-}2, 8\text{e-}2, 9\text{e-}2, 1\text{e-}1\}$, https://github.com/bvarici/intervention-estimation
- **PreDITEr** - $\lambda_{l1} \in \{1\text{e-}1, 3\text{e-}1\}$, $\lambda_{pasp} \in \{1\text{e-}1, 2\text{e-}1\}$, https://github.com/bvarici/uai2022-intervention-estimation-latents

In addition to our selected baselines, we also enumerate other classic baselines relevant to causal discovery from intervention and explain why they were not chosen for our study:

- **DCDI:** This method is a well-known and widely used approach for causal discovery using neural networks, relying on normalizing flows as a generic density estimator. Therefore, it is primarily applicable to continuous data types. We found in experimental testing that it almost never converges and operates at an unbearably slow pace in the case of discrete data. Hence, we disregard its results.
- **SDI:** This method is the first to use neural networks and adapt to discrete data types for intervention causal discovery. However, due to its high complexity, it is often challenging to scale to large-scale node graphs. Additionally, according to the original repository code, its hybrid C-language requirement for compiler adaptation leads to abnormal errors. Hence, we disregard its results.
- **CSIvA:** The lack of accessible code and complex parameter settings make it impossible to replicate the findings of the paper.
- **BaCaDI:** Similar reasons to DCDI.
- **LIT:** Similar reasons to CSIvA.

E.3 Metrics

We design different reasonable metrics for two different tasks, *i.e.*, $\mathcal{I}$-CPDAG discovery and intervention target detection. The detailed introduction is as follows:

$\mathcal{I}$-CPDAG discovery. We first calculate Structural Hamming Distance (SHD) at $\mathcal{I}$-CPDAG level. Specifically, SHD is computed between the learned $\mathcal{I}$-CPDAG($\hat{\mathcal{G}}$) and ground truth $\mathcal{I}$-CPDAG($\mathcal{G}$), *i.e.*, the smallest number of edge additions, deletions, direction reversals and type changes (directed vs. undirected) to convert the output $\mathcal{I}$-CPDAG to ground truth $\mathcal{I}$-CPDAG. As is shown in Table 8, SHD is equal to the sum of the number of ✗s in the table.

Table 8: SHD calculation details.

in Predict→ in Ground-Truth↓	identifiable (directed)		unidentifiable (undirected)	missing in skeleton
	right	wrong		
identifiable	① ✓	② ✗	③ ✗	④ ✗
unidentifiable	⑤ ✗		⑥ ✓	⑦ ✗
nonexist	⑧ ✗		⑨ ✗	⑩ ✓

Different graphs may lead to different causal inference statements and different intervention distributions. To quantify this discrepancy, we use the (pre-) distance between $\mathcal{I}$-CPDAG($\hat{\mathcal{G}}$)s, known as Structural Intervention Distance (SID). The SID is solely based on graphical criteria and quantifies the closeness between two causal graphs according to their corresponding causal inference statements. Thus, it is highly suitable for assessing graphs used for the computation of interventions. Formally:

$$\begin{aligned}\text{SID} : (\hat{\mathcal{G}}, \mathcal{G}) \;\mapsto\; & \#\{(i,j), i \neq j |\; the\ intervention\ distribution\ from\ i\ to\ j \\ & \qquad\qquad is\ falsely\ estimated\ by\ \hat{\mathcal{G}}\ with\ respect\ to\ \mathcal{G}\}\end{aligned}$$

For more detailed calculation algorithms, we recommend readers to refer to (Peters & Bühlmann, 2015) carefully.

F1-score is then calculated based on the identifiable edges of $\mathcal{I}$-CPDAG($\hat{G}$) and $\mathcal{I}$-CPDAG(G), where the accuracy (precision) is equal to True Positive Rate (TPR) and the recall (recall) is equal to 1 - False Discovery Rate (FDR). Details about the specific calculation can also refer to Table 8:

$$\text{Precision} = \text{TPR} = \frac{\text{①}}{\text{①} + \text{②} + \text{③} + \text{④}},$$

$$\text{Recall} = 1 - \text{FDR} = \frac{\text{①}}{\text{①} + \text{②} + \text{⑤} + \text{⑧}},$$

$$\text{F1-Score} = \frac{2 \times \text{Precision} \times \text{Recall}}{\text{Precision} + \text{Recall}},$$

Intervention Target Detection. We then use the F1-Score metric to measure the detection of intervention targets. Let the set of all intervention family edges be denoted as $\hat{\mathcal{I}}$, and all predicted intervention target edges be denoted as $\mathcal{I}$. Then we can formally define:

$$\text{Precision} = \frac{\#(\mathcal{I} \cap \hat{\mathcal{I}})}{\#\mathcal{I}},$$

$$\text{Recall} = \frac{\#(\mathcal{I} \cap \hat{\mathcal{I}})}{\#\hat{\mathcal{I}}},$$

$$\text{F1-Score} = \frac{2 \times \text{Precision} \times \text{Recall}}{\text{Precision} + \text{Recall}}.$$

E.4 Experiments Setting

Computational Resources. For conducting experiments in this work, we employed the IS-MCMC algorithm to pre-generate training data for each test dataset. Subsequently, we trained two types of models, namely the skeleton model and the orientation model, based on the data. The skeleton model comprises multiple cascaded models, with a default maximum of 4 order. Our benchmark environment consists of a Linux server equipped with a 1× AMD EPYC 7763 128-Core Processor CPU (512GB memory) and 4× NVIDIA RTX A6000 (48GB memory) GPUs. To carry out benchmark testing experiments, all baselines are set to run for a duration of 12 hours by default, with specific timings contingent upon the method. It is noteworthy that our method does not necessitate GPU computation, although optimization may further expedite processes. Other methods, depending on their implementation choices, may opt for GPU acceleration.

Table 9: Basic configuration of our experiments and methods

Category	Detail	Hyperparameters or Settings
Training Data	#Training Instances	400 (default) 100 $\sim$ 1600 (others, see 4.2)
	#Simples / per Instance	10k (default) 1k $\sim$ 20k (others, see 4.2)
Testing Data	#Observation Sample	10k (default) 2k $\sim$ 10k (others, see F.2.2)
	#Intervention Sample	10k (default) 1k $\sim$ 10k (others, see F.2.1)
Intervention Experiment	Intervention Type	Single + Soft + Unknow (default) Single + Hard + Unknow (others, see F.1.1) Multiple + Soft + Unknow (others, see F.1.2)
	#Intervention Exp.	#Var. × 0.2 (default) #Var. × {0.0, 0.4, 0.8} (others, see F.3)
Initial Graph Seed	Proxy Algorithm	JCI-BLIP (default) Random Graph (others, see 4.2)
Model threshold	Skeleton Threshold Orientation Threshold	0.5 $\sim$ 0.75 0.1

Basic Configurations. As shown in Table 9, we provide the basic parameter configurations for our TICL, along with the fundamental details of the synthetic data and test data used in various types of experiments in this paper. Furthermore, we provide some basic conceptual explanations. The training data refers to the pre-sampled synthetic data, which includes pairs of instances used for training. These pairs consist of re-parameterized synthetic graphs and sample data tables obtained through forward sampling based on conditional probability tables. As for the test data, we directly retrieve the causal graph structure and parameterized conditional probability tables from bnlearn. Then, the data obtained directly through forward sampling is referred to as observed samples. Otherwise, we can conduct various types of intervention experiments, including single-node intervention or multi-node intervention (*i.e.*, intervening on one or multiple nodes at a time), soft intervention or hard intervention (*i.e.*, whether to eliminate dependencies of parent nodes; for soft intervention, we replace probability distributions sampled from the Dirichlet distribution with parameters $\alpha \sim U[0.2, 1.0]$), and known intervention or unknown intervention targets (*i.e.*, whether we have prior knowledge of intervention target nodes). For the starting point of IS-MCMC sampling, we default to selecting JCI+BLIP as the proxy algorithm to obtain the initial graph seed. We use the `xgb.XGBClassifier()` API provided by Scikit-learn[4] as the classifier for both skeleton and orientation models. Different threshold parameters are set for skeleton identification and orientation identification, while all other hyper-parameters are set to default values. The source code of our method is available at https://anonymous.4open.science/r/iSCL-081D

[4] https://scikit-learn.org/stable/

F Additional Experiments (RQ4)

F.1 Effect of Intervention Type

F.1.1 Prefect Interventions

We follow the default parameter settings, replacing soft interventions with hard interventions, *i.e.*, perfect interventions, to eliminate the dependency of the parent node. The results of $\mathcal{I}$-CPDAG structure discovery are shown in Table 10, and the results of intervention target identification are shown in Table 11. The results indicate that our method consistently outperforms on almost all datasets and metrics.

Table 10: Performance comparison of $\mathcal{I}$-*CPDAG* under perfect intervention (F1 Score ↑ / SHD ↓ / SID ↓). ♣: Crashes, ♠: Timeout.

Datasets #nodes / #edges	Metric	TICL	JCI-GOLEM	JCI-PC	JCI-BLIP	JCI-HC	AVICI*	ENCO*	IGSP*	GIES	UT-IGSP
Earthquake **5 / 4**	F1 Score	**1.00**	0.00	**1.00**	**1.00**	0.00	0.29	0.67	**1.00**	**1.00**	**1.00**
	SHD	**0**	6	**0**	**0**	4	4	2	**0**	**0**	**0**
	SID	**0**	13	**0**	**0**	20	10	2	**0**	**0**	**0**
Survey **6 / 6**	F1 Score	**1.00**	0.40	0.40	0.73	0.73	0.00	0.44	0.91	0.91	0.91
	SHD	**0**	7	4	2	2	6	4	1	1	1
	SID	**0**	23	18	9	9	17	16	4	4	4
Asia **8 / 8**	F1 Score	**0.86**	0.00	0.40	**0.86**	0.12	0.00	0.22	0.77	0.71	0.43
	SHD	**2**	14	8	**2**	13	8	10	3	4	6
	SID	12	36	34	**12**	47	34	28	**10**	18	24
Sachs **11 / 17**	F1 Score	**0.79**	0.00	0.44	**0.79**	0.71	♣	0.25	0.56	0.51	0.56
	SHD	**6**	20	17	**6**	8	♣	36	13	18	13
	SID	**27**	61	30	**27**	29	♣	35	28	34	32
Child **20 / 25**	F1 Score	**0.76**	0.24	0.25	0.75	0.65	♣	0.07	0.49	0.38	0.53
	SHD	**10**	34	45	11	16	♣	105	29	53	29
	SID	160	301	233	188	226	♣	210	125	140	**112**
Insurance **27 / 52**	F1 Score	**0.72**	0.15	0.47	0.71	0.47	♣	0.11	0.37	0.39	0.37
	SHD	**22**	73	64	24	43	♣	171	77	96	78
	SID	325	671	414	390	421	♣	536	442	**316**	452
Water **32 / 66**	F1 Score	**0.58**	0.14	♠	0.50	0.30	♣	0.24	♣	♣	♣
	SHD	**42**	77	♠	44	71	♣	80	♣	♣	♣
	SID	**419**	566	♠	457	642	♣	508	♣	♣	♣

Table 11: Performance comparison of *Intervention Targets Detection* under perfect intervention (F1 Score ↑). ♣: Crashes, ♠: Timeout.

Datasets	**Earthquake**	**Survey**	**Asia**	**Sachs**	**Child**	**Insurance**	**Water**
	1	1	2	2	4	5	6
UT-IGSP	0.40	0.50	0.44	0.40	0.36	0.22	♣
CITE	**1.00**	**1.00**	**1.00**	0.57	0.40	0.55	♣
PreDITEr	0.67	♣	**1.00**	0.67	♠	♠	♣
JCI-GOLEM	0.67	**1.00**	0.00	0.18	0.22	0.28	0.21
JCI-HC	0.50	**1.00**	0.36	0.67	0.47	0.34	0.32
JCI-BLIP	**1.00**	**1.00**	0.80	0.80	0.53	0.44	0.42
JCI-PC	**1.00**	0.67	0.67	0.47	0.47	0.45	♠
TICL	**1.00**	**1.00**	**1.00**	**1.00**	**1.00**	**1.00**	**1.00**

F.1.2 Multiple Interventions

Next, we consider conducting multi-node interventions, where for each intervention experiment, we randomly select 1 to 3 nodes for intervention, with the selection of nodes being without replacement, while the rest follow the default parameter settings. The results of $\mathcal{I}$-CPDAG structure discovery are shown in Table 12, and the results of intervention target identification are shown in Table 13. The results indicate that our method still maintains a consistent lead in almost all datasets and metrics. Additionally, it is worth noting that in the case of interventions on multiple nodes simultaneously, we observed that the performance does not necessarily improve compared to single-node interventions, which may be due to the complexity introduced by intervening on multiple nodes at the same time.

Table 12: Performance comparison of *$\mathcal{I}$-CPDAG* under multiple interventions (F1 Score ↑ / SHD ↓ / SID ↓). ♣: Crashes, ♠: Timeout.

Datasets #nodes / #edges	Metric	TICL	JCI-GOLEM	JCI-PC	JCI-BLIP	JCI-HC	IGSP*	GIES	UT-IGSP
Earthquake **5 / 4**	F1 Score	0.60	0.00	0.55	**1.00**	0.25	**1.00**	0.40	**1.00**
	SHD	4	5	4	**0**	6	**0**	7	**0**
	SID	9	18	3	**0**	15	**0**	6	**0**
Survey **6 / 6**	F1 Score	0.83	0.00	0.40	**0.91**	0.83	**0.91**	0.00	**0.91**
	SHD	2	9	4	**1**	**1**	**1**	6	**1**
	SID	10	30	18	**4**	6	**4**	30	**4**
Asia **8 / 8**	F1 Score	0.86	0.08	0.56	**0.95**	0.56	0.46	0.44	0.77
	SHD	2	9	7	**1**	7	5	7	3
	SID	8	33	17	**5**	21	20	25	10
Sachs **11 / 17**	F1 Score	**0.94**	0.16	0.56	0.90	0.54	0.51	0.32	0.72
	SHD	**2**	18	12	3	12	14	19	10
	SID	**8**	61	38	21	48	35	43	15
Child **20 / 25**	F1 Score	**0.61**	0.18	0.26	0.60	0.44	0.60	0.33	0.51
	SHD	**14**	44	45	15	24	25	47	29
	SID	243	308	229	251	304	**72**	170	117
Insurance **27 / 52**	F1 Score	**0.73**	0.16	0.36	0.69	0.52	0.34	0.45	0.33
	SHD	**22**	63	72	27	38	81	85	81
	SID	369	624	472	398	425	470	**276**	453
Water **32 / 66**	F1 Score	**0.62**	0.20	♠	0.60	0.24	♣	♣	♣
	SHD	**39**	81	♠	42	71	♣	♣	♣
	SID	**436**	605	♠	478	655	♣	♣	♣

Table 13: Performance comparison of *Intervention Targets Detection* under multiple interventions (F1 Score ↑). ♣: Crashes, ♠: Timeout.

Datasets	**Earthquake**	**Survey**	**Asia**	**Sachs**	**Child**	**Insurance**	**Water**
	3	3	6	6	4	5	12
UT-IGSP	0.86	0.86	0.67	0.57	0.80	0.24	♣
CITE	0.80	**1.00**	0.67	0.43	0.33	0.71	♣
PreDITEr	0.80	0.50	♣	0.29	♠	♠	♣
JCI-GOLEM	0.33	0.80	0.62	0.47	0.21	0.14	0.23
JCI-HC	0.57	**1.00**	0.67	0.67	0.50	0.33	0.38
JCI-BLIP	**1.00**	**1.00**	0.86	**0.86**	0.44	0.42	0.57
JCI-PC	0.80	**1.00**	0.92	0.75	0.50	0.33	♠
TICL	0.80	**1.00**	**1.00**	**0.86**	**1.00**	**0.86**	**1.00**

F.2 Effect of Sample Size

F.2.1 Limited interventional data sample sizes

Intervention experiments in the real world are often unrealistic or costly, such as gene knockout experiments, where only a small amount of experimental data may be available. Therefore, we further consider the case of limited intervention data sample size. Specifically, we reduce the sample size of each intervention experiment from 10,000 to 1,000 to simulate this scenario, while keeping other parameters at their default settings. The results of $\mathcal{I}$-CPDAG structure discovery are shown in Table 14, and the results of intervention target identification are shown in Table 17. The results indicate that most methods show a certain degree of performance decline. Nevertheless, our method still maintains a significant lead on almost all datasets and metrics, demonstrating the robustness and superiority of our `TICL` approach.

Table 14: Performance comparison of $\mathcal{I}$*-CPDAG* under limited interventional data sample sizes (F1 Score ↑ / SHD ↓ / SID ↓). ♣: Crashes, ♠: Timeout.

Datasets #nodes / #edges	Metric	`TICL`	JCI-GOLEM	JCI-PC	JCI-BLIP	JCI-HC	AVICI*	ENCO*	IGSP*	GIES	UT-IGSP
Earthquake **5 / 4**	F1 Score	**1.00**	0.00	0.89	**1.00**	**1.00**	0.00	0.67	**1.00**	**1.00**	**1.00**
	SHD	**0**	7	1	0	1	4	2	**0**	**0**	**0**
	SID	**0**	12	**0**	**0**	**0**	10	2	**0**	**0**	**0**
Survey **6 / 6**	F1 Score	0.73	0.00	0.33	0.73	0.00	0.00	0.60	**0.91**	**0.91**	**0.91**
	SHD	2	11	6	2	7	5	3	**1**	**1**	**1**
	SID	9	30	22	9	30	17	14	**4**	**4**	**4**
Asia **8 / 8**	F1 Score	**0.80**	0.20	0.33	**0.80**	0.33	0.00	0.70	0.77	0.71	0.77
	SHD	**3**	11	7	**3**	11	8	6	**3**	4	**3**
	SID	**8**	38	38	19	34	37	9	10	18	10
Sachs **11 / 17**	F1 Score	**0.74**	0.00	0.44	0.21	0.38	0.08	0.17	0.67	0.32	0.62
	SHD	**7**	23	17	15	13	17	41	11	21	12
	SID	31	62	42	55	48	60	47	**24**	40	30
Child **20 / 25**	F1 Score	**0.80**	0.16	0.25	0.75	0.54	0.56	0.14	0.51	0.47	0.49
	SHD	**10**	41	39	**10**	20	16	96	28	36	28
	SID	168	315	277	185	249	188	192	128	**125**	135
Insurance **27 / 52**	F1 Score	**0.64**	0.06	0.37	0.60	0.57	0.17	0.12	0.30	0.53	0.38
	SHD	**25**	65	66	**25**	37	51	162	82	58	75
	SID	395	677	544	404	423	625	539	451	**246**	438
Water **32 / 66**	F1 Score	**0.47**	0.19	♠	0.40	0.45	♣	**0.47**	♣	♣	♣
	SHD	**47**	71	♠	51	52	♣	53	♣	♣	♣
	SID	496	545	♠	540	**398**	♣	473	♣	♣	♣

Table 15: Performance comparison of *Intervention Targets Detection* under limited interventional data sample sizes (F1 Score ↑). ♣: Crashes, ♠: Timeout.

Datasets	**Earthquake**	**Survey**	**Asia**	**Sachs**	**Child**	**Insurance**	**Water**
	1	1	2	2	4	5	6
UT-IGSP	0.33	**1.00**	0.57	**1.00**	0.36	0.27	♣
CITE	**1.00**	0.67	0.67	**1.00**	0.40	0.22	♣
PreDITEr	0.67	**1.00**	♣	0.40	0.33	♠	♣
JCI-GOLEM	0.00	**1.00**	0.00	0.27	0.15	0.11	0.00
JCI-HC	**1.00**	0.67	0.50	0.80	0.40	0.37	0.36
JCI-BLIP	**1.00**	**1.00**	0.67	0.67	0.40	0.44	0.40
JCI-PC	**1.00**	**1.00**	0.67	0.80	0.44	0.32	♠
`TICL`	**1.00**	**1.00**	**1.00**	**1.00**	**1.00**	**0.91**	**1.00**

F.2.2 Limited observational data sample sizes

Similarly, we also consider the case of limited sample size of observational data. Specifically, we reduce the sample size of the observational data from 10,000 to 2,000 to simulate this scenario, while keeping the rest of the parameters at their default settings. The results of $\mathcal{I}$-CPDAG structure discovery are shown in Table 16, and the results of intervention target identification are shown in Table 17. The results are similar, indicating the importance of observational data for causal structure identification. We also see that our method is still in a good leading position.

Table 16: Performance comparison of *$\mathcal{I}$-CPDAG* under limited observational data sample sizes (F1 Score ↑ / SHD ↓ / SID ↓). ♣: Crashes, ♠: Timeout.

Datasets #nodes / #edges	Metric	TICL	JCI-GOLEM	JCI-PC	JCI-BLIP	JCI-HC	AVICI*	ENCO*	IGSP*	GIES	UT-IGSP
Earthquake **5 / 4**	F1 Score	0.86	0.00	0.86	**1.00**	**1.00**	0.17	0.57	**1.00**	0.00	**1.00**
	SHD	1	6	1	**0**	**0**	8	3	**0**	4	**0**
	SID	1	16	1	**0**	**0**	13	2	**0**	16	**0**
Survey **6 / 6**	F1 Score	**0.73**	0.00	0.40	**0.73**	0.29	0.00	0.25	0.50	0.36	0.50
	SHD	**2**	12	4	**2**	6	7	5	4	4	4
	SID	**11**	30	18	9	29	22	18	**11**	20	**11**
Asia **8 / 8**	F1 Score	**0.77**	0.00	0.29	0.67	0.53	0.38	0.71	**0.77**	0.40	**0.77**
	SHD	4	10	7	4	5	8	4	**3**	6	**3**
	SID	18	46	39	18	31	34	14	**10**	42	**10**
Sachs **11 / 17**	F1 Score	0.45	0.09	0.63	0.21	0.36	0.27	0.25	**0.65**	0.35	0.47
	SHD	12	17	13	15	14	14	29	**9**	22	12
	SID	49	54	24	55	53	57	45	**18**	37	39
Child **20 / 25**	F1 Score	**0.75**	0.20	0.17	0.62	**0.75**	♣	0.11	0.69	0.38	0.65
	SHD	**10**	44	50	17	11	♣	110	16	53	17
	SID	181	290	258	266	186	♣	220	**62**	139	99
Insurance **27 / 52**	F1 Score	0.61	0.20	0.38	**0.62**	0.52	♣	0.15	0.54	0.41	0.56
	SHD	**29**	69	64	30	38	♣	127	40	89	39
	SID	424	630	538	451	453	♣	540	364	**347**	428
Water **32 / 66**	F1 Score	**0.50**	0.21	♠	0.49	0.35	♣	0.40	♣	♣	♣
	SHD	**44**	81	♠	46	61	♣	57	♣	♣	♣
	SID	**507**	620	♠	510	532	♣	527	♣	♣	♣

Table 17: Performance comparison of *Intervention Targets Detection* under limited observational data sample sizes (F1 Score ↑). ♣: Crashes, ♠: Timeout.

Datasets	**Earthquake**	**Survey**	**Asia**	**Sachs**	**Child**	**Insurance**	**Water**
	1	1	2	2	4	5	6
UT-IGSP	0.33	0.67	0.40	0.67	0.81	0.24	♣
CITE	♣	**1.00**	♣	**1.00**	0.33	0.38	♣
PreDITEr	♣	**1.00**	♣	♣	0.40	♠	♣
JCI-GOLEM	0.00	0.00	0.00	0.27	0.15	0.27	0.20
JCI-HC	**1.00**	0.67	0.44	0.50	0.57	0.37	0.30
JCI-BLIP	**1.00**	**1.00**	0.67	0.67	0.44	0.44	0.37
JCI-PC	**1.00**	0.67	0.40	0.57	0.29	0.30	♠
TICL	**1.00**	0.67	**1.00**	**1.00**	**0.86**	**0.59**	**1.00**

F.3 Effect of Intervention Experiment Size

Finally, we investigated the impact of different intervention trial frequencies on causal structure discovery. Specifically, we set intervention frequencies at 0%, 20%, 40%, and 80% of the target graph nodes, where 0% means inferring causal structure solely from observational data. We conducted experiments on the Child dataset (20 nodes) using seven methods, including ours, and the results of I-CPDAG structure discovery at different intervention frequencies are shown in Figure 13. The experiments align with intuition, showing that with an increasing number of experiments, all methods exhibit improvements in various metrics, with our method standing out more prominently.

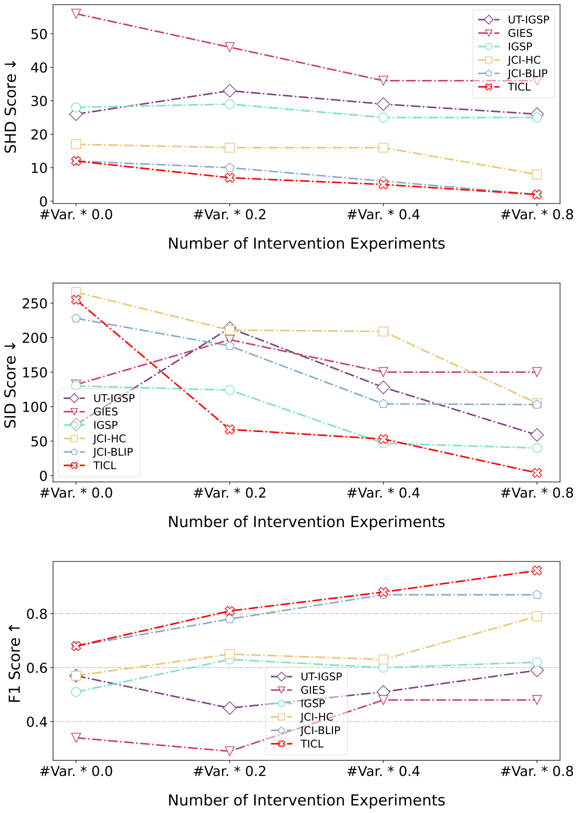

Figure 13: Exploration of the impact of different size of intervention experiments on performance

G More Related Work

Causal Discovery From Observational Data. Traditional causal discovery algorithms infer causal structures from static observational data and fall into four types: constraint-based, score-based, gradient-based, and function causal model methods. Constraint-based algorithms, such as PC (Spirtes & Glymour, 1991), FCI (Spirtes et al., 2000), and PC-Stable (Colombo et al., 2014), utilize conditional independence relations inferred from the faithfulness assumption to establish graphical separations. Coupled with reliable conditional independence testing, these methods handle diverse data distributions and causal relations but are limited to identifying partial DAG. Score-based algorithms search for the optimal DAG under combination constraints using predefined scoring functions. Examples include GES (Chickering, 2002b), hill climbing (Koller & Friedman, 2009), and integer programming (Cussens, 2012). Gradient-based methods extend score-based approaches by transforming discrete search into continuous equality constraints. For example, NOTEARS (Zheng et al., 2018) utilizes algebraic features of DAGs for a smooth global search, but assumes linear relations. GAE (Ng et al., 2019), GraN-DAG (Yu et al., 2019) and SG-MCMC (Annadani et al., 2023) extend this to non-linear functions. Other models relax constraints (Ng et al., 2020) and use reinforcement learning (Wang et al., 2021) as a complement. Function causal model methods like LiNGAM (Comon,

1994) and ANM (Hoyer et al., 2008) describe causal relations in specific functional forms, differentiating between DAGs within the same equivalence class with additional assumptions on data distribution or function classes. *Nevertheless, the identifiability of structures obtained solely from observational data without specific assumptions is theoretically limited.*

Causal Discovery From Interventional Data. Despite the potential identifiability of Directed Acyclic Graphs (DAGs) under sufficient *i.i.d.* interventions and certain assumptions, limited literature explores this problems due to the diversity in types and strategies of intervention data. GIES (Hauser & Bühlmann, 2012) extends the GES algorithm to intervention settings by leveraging the similarity between observed causal graphs and their corresponding intervened graphs. It follows the same two-step approach as the original process, utilizing forward and backward stage traversal through the search space until achieving local maximum scores. Focusing on perfect interventions, IGSP (Wang et al., 2017; Yang et al., 2018) introduces a greedy sparse permutation method, offering an extension to general interventions. This involves optimizing the scoring function through a greedy approach and guiding permutation-based strategies for traversing the $\mathcal{I}$-MEC space. Subsequently, UT-IGSP (Squires et al., 2020) partially addresses unknown target intervention scenarios. Recently, ENCO (Lippe et al., 2022), based on the concept of invariance, proposes a continuous optimization method to learn causal structures from intervention data, modeling the existence of edges and edge direction as separate parameters. *Nonetheless, all of these methods typically focus on a limited set of intervention scenarios and fail to provide a unified approach for effectively addressing the problem of causal discovery from interventions.*

Supervised Causal Discovery. Supervised causal discovery aims to pre-access synthetic datasets of causal relations and learn causal directions in a supervised manner. Early research focused on pairwise relations, including RCC (Lopez-Paz et al., 2015) and MRCL (Hill et al., 2019). For multivariate causal learning, DAG-EQ (Li et al., 2020), based on permutation-equivariant edge models, investigated supervised causal discovery using synthetic data from linear causal models, showing promising results. Subsequently, SLdisco (Petersen et al., 2022) address shortcomings in sample size and graph density settings. It trained on synthetic linear Gaussian data to learn equivalence classes of causal graphs from observational datasets. Recently, CSIvA (Ke et al., 2023b) devised a transformer architecture with permutation invariance, extending the supervised learning paradigm to incorporate intervention data for increased flexibility. Concurrently, AVICI (Lorch et al., 2022), leveraging amortized variational inference optimization, circumvented the challenges of structural search to predict causal structures directly from the provided dataset. Considering that the aforementioned methods only evaluate a limited set of real causal model data and may not effectively capture fundamental causal information, such as persistent dependencies (Yu et al., 2016) and directional asymmetry. ML4S (Ma et al., 2022) and ML4C (Dai et al., 2023), operating under the supervised paradigm for skeleton and direction learning, achieved progressively significant identifiability. *However, causal discovery for various types of intervention data scenarios remains inadequately addressed in the supervised paradigm. Our approach represents the first unified solution for supervised intervention causal discovery.*

H More Discussion

H.1 Supervised Causal Discovery

We advocate for causal discovery from intervention data in supervised paradigm. Identifiable causal relationships between causal graphs can be treated as ground truth labels, and corresponding data can be obtained through forward sampling. Importantly, this sampling strategy is cost-free, allowing us to obtain an infinite number of samples for training a model to compress the mapping between data and causal relationships. As the main study on data quantity, typically, the more data, the better performance. Furthermore, although we can freely generate parameterized causal graphs, for specific systems of interest, such as the aforementioned study on data quality, we consider training data derived using posterior distributions to be useful for causal discovery of the data of interest.

H.2 Self-augmentation *vs.* Pre-training

We noticed that all the SCL methods in the literature, during the training phase, integrate or generate datasets containing various causal mechanisms and their related data samples through simulators (if available), however, such generation mechanisms are entirely dependent on manual specification. Ideally, it is preferable to predefine rich synthetic graph structures (possible examples include ER / SF / Low Rank / Random graphs, etc.) and synthetic function types (including linear, quadratic, nonlinear, etc.) as much as possible. We refer to the process of synthesizing data during the training phase and then training them together as ”pre-training”, similar to today’s language model pre-training, using massive training data to achieve generalization in different domains. However, causal structure learning is a high-risk field, where people often pay more attention to performance. The potential danger of this pre-training method is that if the causal mechanisms of the system of interest have never been seen before, there may be out-of-distribution generalization issues. Therefore, in this paper, we advocate acquiring training data more relevant to the test data after accessing the test data, providing high-quality training data by observing the posterior estimates of causal graphs to avoid the ”domain shift” problem. We call this self-augmentation method, similar to in-context learning, adjusting on specific testing instance of interest in order to achieve high performance that is usable.

H.3 Discrete *vs.* Continuous Data

In this paper, we mainly focus on causal structure identification from discrete data. The *Markov completeness* theorem states that for discrete or linear Gaussian data, we can only identify causal graphs up to their CPDAG. For continuous data satisfying linear non-Gaussian mechanisms or additive noise assumptions, we can identify more causal directions. However, our goal is to properly handle intervention data by using a supervised learning paradigm to learn identifiable causal structures. Therefore, more considerations may be needed to design corresponding learning tasks for continuous data. Nevertheless, in practice, our method can be naturally extended to continuous data by utilizing standard algorithms from existing literature, such as the Hilbert-Schmidt Independence Criterion (Gretton et al., 2007) to compute conditional dependencies of numerical variables. Despite this, more attention may need to be paid, which we consider as future work.

I Broader Impacts

We propose TICL, a new method for causal discovery from data with unknown intervention targets. Specifically, we introduce the concept of self-augmentation, using test data to obtain high-quality usable synthetic training data and identifying causal structures under the paradigm of supervised learning. Additionally, we advocate for joint causal inference as a fundamental framework for handling different intervention settings. Our numerical experiments demonstrate that our method outperforms existing intervention causal discovery methods on a wide range of datasets and metrics. However, despite the existence of supervisory identifiability, due to our adoption of traditional manual feature engineering, certain features may incur negative returns in specific situations for the final causal identifiability judgment. Therefore, future work will explore extending it to fully end-to-end neural network models, which may be more suitable by automatically capturing features instead of manual operations. Finally, as a potential benefit of the design of joint causal reasoning, we can naturally identify unknown intervention targets while discovering causality, enabling scientists to apply these methods to automated experiment design and scientific discovery.